Conf-941124--22

PNL-SA-24505

ABIOTIC REDUCTION OF AQUIFER MATERIALS BY DITHIONITE: A PROMISING IN-SITU REMEDIAITON TECHNOLOGY

J. E. Amonette
J. E. Szecsody
H. T. Schaef
J. C. Templeton[a]
Y. A. Gorby
J. S. Fruchter

November 1994

Presented at the
Thirty-Third Symposium on Health & the Environment In Situ Remediation:
Scientific Base for Current & Future Technologies
November 7-11, 1994
Richland, Washington

Prepared for
the U.S. Department of Energy
under Contract DE-AC06-76RLO 1830

Pacific Northwest Laboratory
Richland, Washington 99352

MASTER

---

[a] Whitman College, Walla Walla, Washington

DISCLAIMER

ABIOTIC REDUCTION OF AQUIFER MATERIALS BY DITHIONITE: A PROMISING IN-SITU REMEDIATION TECHNOLOGY

J. E. Amonette,[1] J. E. Szecsody,[1] H. T. Schaef,[1] J. C. Templeton,[2] Y. A. Gorby,[1] and J. S. Fruchter[1]

[1]Pacific Northwest Laboratory, Richland, Washington
[2]Whitman College, Walla Walla, Washington

Key Words: Sodium dithionite, iron reduction, tetrachloromethane, in-situ remediation, abiotic remediation

Running Head: Abiotic Remediation with Dithionite

ABSTRACT

Laboratory batch and column experiments were conducted with Hanford sediments to develop the capability to predict (1) the longevity of dithionite in these systems, (2) its efficiency as a reductant of structural iron, and (3) the longevity and reactivity of the reduced iron with soluble inorganic and organic species. After an initial induction period, the loss of dithionite by disproportionation and oxidation could be described by pseudo-first-order (PFO) kinetics. Other than the initial reaction with ferric iron, the primary factor promoting loss of dithionite in this system was disproportionation via heterogeneous catalysis at mineral surfaces. The efficiency of the reduction of structural iron was nearly 100% for the first fourth of the ferric iron, but declined exponentially with higher degrees of reduction so that, at most, 75% of the ferric iron could be reduced. This decrease in reduction efficiency probably was related to differences in the accessibility of ferric iron in the mineral particles, with iron in clay-sized particles being the most accessible and that in silt- and sand-sized particles less accessible. Flow-through column studies showed that a reduced-sediment barrier created in this manner could maintain a reducing environment for about 80 pore volumes

before being reoxidized by groundwater. These experiments also showed that the kinetics of reoxidation were rapid and, consequently, that equilibrium chemistry could be assumed for typical natural flow rates in the Hanford unconfined aquifer. In addition to reaction with oxygen, which was a surrogate for oxidized inorganic species such as chromate, the reduced structural iron also reacted readily with tetrachloromethane. The results of these laboratory experiments suggest that dithonite has excellent promise for use as a reductant in oxidizing aquifers that contain iron-bearing clay minerals and that these minerals, once reduced, are quite effective in removing oxidized species from groundwater.

INTRODUCTION

Manipulation of the reduction-oxidation (redox) status of an aquifer is a possible approach for in-situ remediation of redox-sensitive groundwater contaminants, such as chromate or tetrachloromethane. The approach involves creating a spatially fixed zone or permeable barrier in the aquifer where the aqueous redox environment, which is maintained by constant contact with redox-sensitive elements in the solid phase, is substantially more reducing (or oxidizing) than elsewhere in the aquifer. When groundwater from other parts of the aquifer enters this zone, the soluble redox-sensitive constituents are reduced (or oxidized). As a consequence of this change in redox status, redox-sensitive contaminants may be destroyed or altered to less mobile or less toxic forms. In essence, the permeable barrier acts as a filter that removes redox-sensitive contaminants from the groundwater that passes through it. The effectiveness of the permeable barrier is determined largely by the relationship between the kinetics of the redox reactions and the rate at which the groundwater passes through it. The longevity of the barrier depends on the groundwater-accessible, redox-buffering capacity of the solids in the aquifer matrix and on the concentration of reactive species in the groundwater entering the barrier. Because iron is the most abundant redox-sensitive element in soils and sediments, it is the dominant contributor to the redox-buffering capacities of most aquifers. Thus, for a reducing barrier in an otherwise oxidizing aquifer, the amount of accessible reduced iron in the solids and the dissolved oxygen content of the groundwater are the main factors affecting the barrier's longevity.

A natural analog to the proposed redox barrier concept has been shown to effectively reduce chromate mobility in a suboxic natural aquifer (Kent et al., 1994). By a study of that field system in further detail through a series of laboratory experiments (Anderson et al., 1994), it was shown that the presence of even a small amount (<10 mg kg^{-1}) of Fe(II) could effectively reduce aqueous chromate. Dechlorination of tetrachloromethane by reactions involving Fe(II) in pyrite and in micaceous minerals has also been reported (Kriegman-King and Reinhard, 1994).

The most accessible forms of iron in soils and sediments occur in those mineral phases having the highest specific surface areas, namely, iron oxyhydroxides and iron-bearing layer silicates. These two types of minerals behave quite differently, however, when the iron in them is reduced to the ferrous state. The oxide phases, which are typically dominated by ferric iron, dissolve when the iron is reduced. If sufficient carbonate is present, siderite (ferrous carbonate) may precipitate. Otherwise the iron is solubilized and will flow with the aquifer water until it is adsorbed or encounters an oxidized zone and is reprecipitated in the ferric form. In contrast, iron in the structures of layer silicates is usually retained in the mineral structure regardless of oxidation state (Stucki, 1988; Scott and Amonette, 1988). The excess positive or negative charge created by the redox reaction is usually balanced by a change in the layer charge of the mineral, i.e., in the number of exchangeable cations adsorbed to the mineral surface. In some instances, the structural iron can be ejected, particularly from layer silicates where iron is the dominant structural cation, and from chlorites that contain an iron hydroxide sheet in the interlayer space. In general, however, the iron in layer silicates remains in the mineral structure when reduced and, consequently, can be used to create a spatially fixed zone that removes redox-sensitive contaminants from groundwater.

Creation of a spatially fixed reduced zone in an aquifer requires treatment with a reagent capable of reducing the structural iron in clay- and silt-sized layer silicates. Furthermore, the reagent must participate in few side reactions and be relatively nontoxic in both its original and its reacted forms. A number of the reagents commonly used in the laboratory that are capable of reducing structural iron do not meet these last requirements (e.g., borohydride and stannous chloride). Reduced-sulfur species, on the other hand, generally yield safe oxidized products such as sulfate, but vary in their reactivity and toxicities. One reduced-sulfur species, dithionite ion ($S_2O_4^{2-}$), is quite effective as a reductant without the side effects that limit the use of most other reductants. Our work has therefore focused on understanding the fundamental chemistry of dithionite ion and the kinetics of its reactions with structural iron in layer silicates and sediments that contain these minerals.

Aqueous Chemistry of Dithionite Ion

The dithionite or hydrosulfite ion, $S_2O_4^{2-}$, may be conceptualized as two sulfoxyl ($SO_2^{\bullet-}$) radicals joined by a 2.39-Å sulfur-sulfur bond (Figure 1). The eclipsed conformation of the ion, in which the oxygens associated with each sulfur (S) atom are bound at rather acute angles relative to each other and in proximity to the oxygens attached to the other S atom, induces considerable strain within the ion. As a consequence, the S-S bond in $S_2O_4^{2-}$ is considerably longer (and hence weaker) than typical S-S bonds (2.00-2.15 Å). This weak link in the $S_2O_4^{2-}$ ion is the key to its chemistry because the ion reversibly dissociates to form two $SO_2^{\bullet-}$ radicals that are strong and highly reactive reductants. Reduction reactions with $S_2O_4^{2-}$, then, typically involve two steps: (1) the dissociation of the ion to yield the $SO_2^{\bullet-}$ radicals and (2) the reaction of the radicals with the oxidized species to yield a reduced species and sulfite (SO_3^{2-}) or bisulfite (HSO_3^-) ions (Figure 2). Because the $SO_2^{\bullet-}$ radicals are extremely reactive, the dissociation of the $S_2O_4^{2-}$ ion is the slow or rate-limiting step in most reactions involving dithionite.

Dithionite is a strong reductant, particularly in strongly basic solutions in which its reduction potential is -1.12 V. From a thermodynamic perspective, $S_2O_4^{2-}$ is capable of reducing water, although the activation energy of the reaction is apparently large enough to keep the rate of the reaction very slow relative to the reduction of other oxidized species. Dithionite also undergoes a disproportionation reaction in aqueous solutions to yield thiosulfate ($S_2O_3^{2-}$) and HSO_3^- ions. As in the reactions with oxidants, cleavage of the S-S bond is required and is presumably the rate-limiting step in the process. Thus, dithionite is not stable in aqueous solutions for long periods.

Determination of aqueous concentrations of dithionite can be done spectrophotometrically by measuring the absorbance of light at 315 nm (Figure 1). The molar absorptivity at this wavelength is about 6900 L mol^{-1} cm^{-1} and is free from interference by other oxidized and reduced sulfur species.

Heterogeneous Chemistry of an In-Situ Reducing Barrier

The creation and operation of an in-situ reducing barrier involves a number of possible electron transfer, precipitation, and adsorption reactions (Figure 2). The barrier is initially formed by the transfer of electrons from dithionite ions in the aqueous phase to iron atoms in the solid phase, most likely via the sulfoxyl radical. The products of this reaction include reduced iron in layer silicates (i.e., clay), aqueous ferrous iron from the iron oxides that dissolve, and sulfite or bisulfite ions from the dithionite that is oxidized. In addition to reacting with ferric iron, the dithionite undergoes disproportionation to yield sulfite and thiosulfate ions as well as protons. The enhanced levels of sulfite and thiosulfate may lead to precipitation of hannebachite ($CaSO_3 \cdot \frac{1}{2}H_2O$) and the thiosulfate analog ($CaS_2O_3 \cdot 2H_2O$) of gypsum ($CaSO_4 \cdot 2H_2O$). The production of protons will lower the solution pH unless they are countered by the presence of buffering agents, such as carbonate and bicarbonate ions. At pH values below about 6, sulfides may form from the disproportionation of thiosulfate, so it is important to maintain a neutral or slightly alkaline pH in solution during barrier formation. Dithionite ions may also be adsorbed to the edges of layer silicates which may affect the rate of formation of the sulfoxyl free radical and the rate of the dithionite disproportionation reaction. In turn, the aqueous ferrous iron released by the dissolution of the iron oxide phases may precipitate as siderite ($FeCO_3$) if sufficiently high levels of carbonate are present, or, if it encounters an oxidized zone, as amorphous iron oxide {e.g., ferrihydrite [$Fe_5O_7(OH)\cdot 4H_2O$]}.

After all of the reactions associated with the creation of the barrier are completed, the reduced iron in the layer silicates remains available to react with soluble oxidized species that enter the barrier by advection and diffusion (Figure 2). For aqueous chromate species, the reaction products would most likely be $Cr(OH)_3$(am) or an adsorbed Cr(III) hydrolysis species such as $Cr(OH)_2^+$. Reaction with chlorinated hydrocarbons (such as tetrachloromethane) would be expected to yield chloride ions and partly or completely dehalogenated forms of carbon. The dissolved oxygen in groundwater is likely to be the dominant oxidized constituent to react with the barrier, and this reaction will consume protons, raising the pH of the groundwater.

EXPERIMENTAL

Reagents and Solutions

Technical-grade sodium dithionite dihydrate was purchased from Aldrich Chemical Co. All other chemicals used were reagent grade. A nitrogen-sparged 10 mM solution of $NaHCO_3$ equilibrated with excess solid $CaCO_3$ for 48 h was used to simulate Hanford groundwater. Actual filtered Hanford groundwater sparged with an 80:20 mixture of nitrogen and carbon dioxide was used for the dechlorination experiment. Residual reductants were removed from the solid samples by three washes with nitrogen-sparged 0.1 M NaCl solutions before determination of the Fe(II) content of the solids.

Sediments

The <2-mm fraction of samples of two sediments collected during well-drilling operations at the 200-West Area on the Hanford Site was used in these experiments. The batch and column studies were performed using a Hanford formation sample from the 31-m (103-ft) depth of Well 299-W15-217. The dechlorination study was performed using a Middle Ringold formation sample from the 72-m (237-ft) depth of Well 299-W11-32. The samples were removed from the core-barrels and placed into 20-L (5-gal) plastic containers. The containers were sealed and brought to the laboratory, where they were stored at room temperature until used. The samples were passed through a 2-mm-pore-size sieve to remove coarse fragments, homogenized by coning and mixing on a large plastic sheet, then returned to their original plastic container for storage at room temperature. These sediments were fine-grained; less than 5% of the original sample failed to pass through the sieve. The homogenized <2-mm sediments were classified as sandy loams and contained about 6 to 8% clay-, 18% silt-, and 74 to 75% sand-sized particles. The mineralogy of the bulk sediments was dominated by quartz and plagioclase feldspar. The clay fraction mineralogy of the two samples differed. The Middle Ringold formation sample was dominated by smectite, with small amounts of illite, vermiculite, chlorite, and kaolinite present. The Hanford formation sample, on the other hand, contained no kaolinite, less smectite, and more illite, vermiculite, and chlorite. The Hanford formation sample contained about 15.8 g Fe(II) kg^{-1} and 12.0 g Fe(III) kg^{-1} for a total iron content of 27.8 g kg^{-1}. The Middle Ringold formation sample contained about 9.9 g Fe(II) kg^{-1} and 20.9 g Fe(III) kg^{-1}, for a total iron content of 30.8 g kg^{-1}.

Analytical Methods

Ferrous iron and total iron were determined using a modified version (Templeton et al., 1994) of the phenanthroline method of Komadel and Stucki (1988). The aqueous concentration of dithionite was determined by the absorbance at 315 nm, using 6900 L mol^{-1} cm^{-1} as the molar absorptivity (Creutz and Sutin, 1974). Dissolved oxygen levels in column influent and effluent were monitored using a flow-through O_2 electrode (Microelectrodes, Inc., Londonderry, NH). Tetrachloromethane and trichloromethane concentrations were determined by gas chromatography.

Batch Studies

A series of batch studies was conducted to assess both the stability of dithionite under different conditions and its efficiency in reducing the Fe(III) in the Hanford formation sediment. In general, the experiments involved 10, 20, or 30 mL of synthetic Hanford groundwater, 0 to 20 g of the <2-mm sediment, 100 mg of $CaCO_3(s)$ added to buffer the pH, and initial $Na_2S_2O_4$ concentrations of about 2, 13, or 60 mM. The experiments were conducted in 50-mL plastic centrifuge tubes at 30°C under a 96% Ar:4% H_2 atmosphere. The water used to prepare the synthetic Hanford groundwater was sparged with the Ar:H_2 gas mixture before addition of the appropriate amount of $NaHCO_3$ and equilibration for 48 h with excess solid $CaCO_3$. Immediately before the experiment, an appropriate amount of dithionite solid was dissolved in the synthetic groundwater and aliquots of this solution were added to the tubes containing sediment and $CaCO_3$. The tubes were tightly capped, shaken to mix the contents well, then suspended in a 30°C water bath. At suitable intervals after introduction of the dithionite solution to the sediment, aliquots of the solution were removed, filtered, and analyzed for dithionite concentration (under anoxic conditions) by absorbance at 315 nm. A number of replicate tubes was set up initially. At each sampling time, sediment in one tube was washed three times with a sparged 0.1 M solution of either $NaHCO_3$ or NaCl to quench the reduction reaction and remove the excess reductants present. The sediment was stored under anoxic conditions until analysis for ferrous and total iron using the modified phenanthroline method could be performed.

Column Studies

A series of one-dimensional column experiments was conducted to quantify the stoichiometry and kinetics of oxidation of Hanford formation sediment that had first been reduced with dithionite. The experiments consisted of pumping an oxygen-saturated solution of synthetic Hanford groundwater through a 2.5-cm-dia by 2- to 5-cm-long glass column packed with reduced sediment; pumping continued until oxygen saturation was achieved at the column outlet. The reduced sediment was not washed initially to remove excess reductants. An high-pressure liquid chromatography pump was used to maintain a constant flow rate (SSI, Cambridge, MA). Other than the sediment, the materials in contact with the fluid were 316L stainless steel, tetrafluoroethylene (pump seals), and glass. The sediment was prereduced by reacting a 60 mM solution of sodium dithionite with soil for 48 h at a solid:solution ratio of 0.75 g mL^{-1}. Oxygen levels were monitored continuously by a flow-through O_2 electrode at the column inlet and two electrodes at the outlet. Electrodes were calibrated before and after each experiment using an oxygen-saturated solution and an oxygen-deficient solution (obtained by bubbling He in water); oxygen levels were checked with a field O_2 method (Chemetrics, Inc., Fort Collins, CO). The influent and effluent pH, as well as effluent electrical conductivity, were also monitored continuously with flow-through electrodes and recorded by a computer using a multifunction analog/digital conversion board.

Transport Modeling

Three transport models that differed in their representation of the physical/chemical rate process were used in this study. A transport model with linear, first-order, reversible sorption was used to represent a single, slow reaction (Parker and van Genuchten, 1984) or a slow surface-diffusion process (Szecsody and Bales, 1989). This model was constrained by four parameters: K_d, which described the lag in oxygen breakthrough compared to water; k_b, which described the first-order reverse rate coefficient ($time^{-1}$); D, which described the longitudinal hydrodynamic dispersion ($length^2$ $time^{-1}$); and t_1, which defined the injection pulse time. A two-region transport model was used to represent a slow reaction occurring in parallel with a fast reaction. In addition to the four parameters for the linear, first-order model, the two-region model was constrained by a fifth parameter, f, which described the fraction of fast reaction sites (1-f = fraction of slow sites). The third model assumed fast kinetics (i.e., an equilibrium chemical process). This model was used to distinguish flow conditions under which the kinetics of the process are important and affect the breakthrough curve shape (i.e., at faster flow velocities) from those conditions under which local equilibrium could be assumed (i.e., at slower flow velocities).

The method by which a transport model is fitted to column data affects the values of the parameters obtained, because several parameters can independently affect the same aspect of the breakthrough curve shape. To accurately determine the rate constant for a slow chemical/physical process (e.g., k_b), all other model parameters must be determined independently. For this study, longitudinal dispersion was first estimated from the particle-size distribution and the average pore-water velocity (Horvath and Lin, 1978), then compared to the value of dispersion obtained from an equilibrium model fitted to the column experiment run at the slowest velocity (where the process would be closest to equilibrium). Because these two values for dispersion agreed, dispersion was calculated for the other column experiments assuming a linear relationship between velocity and dispersion (Rose, 1977). The total mass of oxygen injected before complete breakthrough was determined by integrating the area in front of the experimental breakthrough curve. This calculation also required an accurate measure of the dry bulk density and porosity, which were obtained from the mass of a soil column packed dry and then saturated and from the column volume.

Dechlorination Study

A batch study using sediment samples from the Middle Ringold formation tested the efficacy of the reduced sediments for destruction of tetrachloromethane. Like the previous batch studies, this experiment was performed at 30°C under an anoxic atmosphere (80% N_2, 15% CO_2, 5% H_2). One gram of the <2-mm sediment was added to each of 24 20-mL-headspace vials inside the anoxic chamber. Forty milligrams of $Na_2S_2O_4$ was added to 12 of the vials. Ten milliliters of a 30 mM $NaHCO_3$ solution that had been sparged with an 80% N_2:20% CO_2 gas mixture was then added to each vial. The vials were sealed and allowed to incubate for 48 h. At the end of this sediment reduction period, the contents of the vials were washed five times with 0.1 M NaCl to remove the excess reductants and then washed three more times with filtered Hanford groundwater.

(Both these solutions had been sparged previously with the N_2:CO_2 gas mixture to remove oxygen.) The reduced and washed sediment was then resuspended in 10 mL of filtered anoxic Hanford groundwater. Tetrachloromethane was added to each vial to yield a final concentration of 0.5 $\mu L\ L^{-1}$, and the vials were immediately sealed with tetrafluoroethylene-coated butyl rubber stoppers. After suitable periods, the loss of tetrachloromethane and the formation of trichloromethane in the vials were determined by gas chromatography.

RESULTS AND DISCUSSION

Decomposition of Dithionite

The initial batch experiment was set up to provide baseline data on the stability of dithionite in synthetic Hanford groundwater when no oxidant (such as iron or oxygen) was present. In this experiment, the only possible causes of dithionite decomposition were its inherent instability (e.g., homogeneous disproportionation to yield sulfite and thiosulfate ions) and interaction with the walls of the centrifuge tubes that might promote the disproportionation reaction by a heterogeneous catalysis mechanism. To distinguish a possible wall effect from the inherent instability of dithionite, replicate samples were run with two volumes of dithionite solution (10 and 30 mL) in the same-sized centrifuge tubes. Stability data for solutions having initial dithionite concentrations of 60 and 2.2 mM were collected.

The results of the baseline experiment showed that the decomposition of dithionite followed PFO kinetics (Figure 3). The 60 mM dithionite solution decomposed at a rate ($t_{1/2}$ = 135 h, k_{app} = 5.1E-3 h^{-1}) that was nearly twice that of the 2.2 mM solution ($t_{1/2}$ = 243 h, k_{app} = 2.9E-3 h^{-1}). This difference may be due to ionic-strength effects; the difference in ionic strength between the two solutions was roughly an order of magnitude. At each concentration, the 10- and 30-mL replicates showed no significant differences suggesting that the contribution of wall effects to the decomposition reaction was negligible.

When in contact with sediments, four reactions were considered to possibly lead to a loss of dithionite. The first of these was the consumption of dithionite by redox reaction with Fe(III). The second reaction was the inherent disproportionation of dithionite as measured in the baseline experiment. The third and fourth possibilities involved homogeneous and heterogeneous catalysis of the dithionite disproportionation reaction by dissolved ions [e.g., Fe(II) released by oxide phases] or by interactions of dithionite and/or sulfoxyl radical with the surfaces of minerals in the sediment. To gain some idea of the relative importance of the redox and possible catalytic reactions, a batch experiment was conducted with sediment samples that were first reduced with dithionite and then washed with 0.1 M $NaHCO_3$ to remove the excess reductants. An identical set of sediment samples received only a deionized-water pretreatment and thus were still in the "oxidized" state before dithionite treatment.

The rates of dithionite decomposition in the presence of the sediment samples (Figure 4) were 5 to 10 times faster than in the baseline experiment with no sediment (Figure 3). Clearly, the presence of the sediment accelerated the rate of dithionite decomposition. The previously reduced sample caused dithonite to decompose at a slightly faster rate ($t_{1/2}$ = 19 h, k_{app} = 3.7E-2 h^{-1}) than did the oxidized sample ($t_{1/2}$ = 24 h, k_{app} = 2.9E-2 h^{-1}), although the rates were not significantly different at the 95% level of probability. Thus, the sediment's acceleration of dithionite decomposition was not due to the reduction of iron by dithionite. Rather, these results provide strong evidence for catalysis of the dithionite disproportionation reaction by the sediment.

Despite the dominant effect of sediment on the disproportionation reaction, oxidation also has some effects in the early stages of the experiment (Figure 5). Between 1 and 6 h of treatment, levels of dithionite were lower in the oxidized sample than in the sample that had been previously reduced. As shown in other experiments (see below), this period coincided with the time when rapid reduction of structural iron occurred, and so the lower level of dithionite in the oxidized sample was expected.

The data in Figure 5 also reveal a period of several hours at the start of the experiment during which the measured dithionite concentration increased, followed by the steady decline in measured dithionite concentration that could be quantified by a PFO rate law. Similar "induction" periods were observed in all the experiments run at initial dithionite concentrations of 60 mM regardless of the presence of sediment, but not in any of the experiments conducted at lower concentrations of dithionite. Since we have high confidence in the initial concentration of dithionite, this phenomenon suggests that the species giving rise to the absorption band at 315 nm is not the dithionite ion, but rather another species derived from it by reaction in aqueous solution. The most likely species is the sulfoxyl radical. If so, then the length of the induction period suggests that equilibrium between the $S_2O_4^{2-}$ and $SO_2^{\bullet -}$ ions (Figure 2) takes several hours to establish at high dithionite concentrations. This phenomenon could occur either because the forward reaction producing the sulfoxyl radical is inhibited or because the radical is consumed so rapidly that it does not accumulate readily. The forward rate constant for the dithionite-sulfoxyl reaction in dilute pH-neutral solution at 25°C has been reported to be about 2.5 s^{-1} (Creutz and Sutin, 1974), which is roughly three orders of magnitude faster than rate constants for the decomposition reactions tested in this study. Because it seems unlikely that sulfoxyl radical production would be inhibited at the start of the experiment when few other ions would be present to cause this inhibition, we suspect that rapid consumption of the sulfoxyl radical occurs until product inhibition slows the consumption rate enough to allow the radical to accumulate. Because all our high-dithionite experiments exhibited this induction period, the PFO rate constants were calculated only for the portion of the data obtained after the induction period.

Further evidence for reactions of dithionite with the sediment surfaces was provided by an experiment comparing the stability of three dithionite solutions having different initial concentrations but in contact with the same quantity of sediment (0.5 solid:solution ratio). If the sediment had no impact on dithionite decomposition rates (i.e., the rate-limiting step of the reaction was strictly homogeneous), the PFO rate constants would be expected to be independent of initial dithionite concentration. On the other hand, for a reaction in which the rate-limiting steps occurred at solid surfaces (i.e., a heterogeneous system), the rate of reaction would be expected to depend on the amount of surface area in contact with the solution.

The initial concentrations (62, 13, and 2.7 mM) were spaced by factors of five. Similarly, the PFO plots of the stability data (Figure 6) yielded decomposition rate constants for dithionite that were also spaced by factors of about five. The most concentrated dithionite solution decayed at the slowest rate ($t_{1/2}$ = 36 h, k_{app} = 1.9E-2 h^{-1}) and the most dilute solution decayed at the fastest rate ($t_{1/2}$ = 1.2 h, k_{app} = 6.0E-1 h^{-1}). Comparison of these rates with those obtained for comparable initial concentrations of dithionite in homogeneous solution (Figure 3) shows that the presence of the sediment increased the rate of dithonite decomposition by 4 to 200 times. The trend in rates with respect to initial dithionite concentration suggested that (1) a limited number of sites controlled the decomposition rate, (2) these sites were saturated by even the lowest concentration of dithionite, and (3) the same sites probably controlled the disproportionation and redox pathways of dithionite decomposition. In other words, although the disproportionation and redox reactions are assumed to operate in parallel, they seem to have the same rate-limiting step--a reaction occurring at a limited number of sites at the sediment particle surfaces.

Dependence of the overall reaction rate on a reaction occurring at a limited number of surface sites could allow interferences from other ions that compete with the dithionite or sulfoxyl ions for adsorption to the surface sites. To test this possibility, several experiments were conducted in which the ionic strength of the solution (i.e., the initial dithionite concentration) was held constant while the number of surface sites (i.e., the amount of sediment contacted) was allowed to vary across a wide range. If no interference occurred, the decomposition rate would be expected to scale in direct proportion to the number of surface sites available. Thus, an increase in the number of surface sites (i.e., in the solid:solution ratio) by a factor of 10 would result in a corresponding 10-fold increase in the decomposition rate. On the other hand, interference by nonparticipating ions would be manifested by a smaller change in the decomposition rate relative to the number of surface sites. To maximize the likelihood of observing such an interference, these experiments were conducted at initial dithionite concentrations of 60 mM.

The results of the solid:solution ratio experiments showed substantial interference in the decomposition of dithionite (Figure 7). A 40-fold increase in the solid:solution ratio produced only a 2-fold increase in the decomposition rate of dithionite. The interference seems to be more pronounced at higher ionic strengths (i.e., higher aqueous concentrations of dithionite). For example, comparison of the dithionite decomposition rates for (1) the experiment at 60 mM initial dithionite concentration and solid:solution ratio of 2.0 in Figure 7, and (2) the experiment at 13 mM initial dithionite concentration and solid:solution ratio of 0.5 in Figure 6 reveal a 3-fold difference, even though the number of moles of dithionite per mass of sediment are roughly the same for the two experiments. Inasmuch as dithionite and the sulfoxyl radical both participate in the decomposition reaction, it seems likely that the interference is caused by one of the anionic products of this reaction, such as sulfite or thiosulfate. These two divalent oxysulfur ions would have affinities for adsorption sites on the sediment surfaces similar to those of dithionite and, thus, would be effective competitors.

Based on these experiments, the kinetics of dithionite decomposition in the aqueous sediment system can be summarized by the following simple rate law:

$$-dC/dt = k_1 C + k_2 C_{surf} C, \tag{1}$$

where C is the concentration of dithionite, t is time, k_1 is the disproportionation rate constant in homogeneous solution, k_2 is the rate constant for the common, rate-determining step in the heterogeneous disproportionation and redox reactions, and C_{surf} is the concentration of available surface sites in the sediment. As we have shown, k_2 is generally >> k_1, and so k_1 may be ignored in rough calculations. The value of C_{surf} will depend on a number of factors, including the mass and mineral composition of the sediment, the type and concentration of competing anions (e.g., sulfite, thiosulfate, hydroxyl, bicarbonate), and the anion exchange capacity of the minerals (largely determined by solution pH). The implicit assumption is that the same minerals that offer adsorption sites for dithionite are reduced by dithionite. It is also implicitly assumed that the contribution of homogeneous catalysis (e.g., from aqueous transition metal ions) is negligible in comparison to the contribution of heterogeneous catalysis. These assumptions are not necessarily correct, and separate terms could be written to account for the two types of heterogeneous reactions, i.e., disproportionation and redox, as well as for the homogeneous catalysis reactions.

Reduction of Sediment Iron

Treatment of the sediment with dithionite solutions resulted in amounts of Fe(III) reduction that ranged from essentially nil to as much as 78% of the Fe(III) originally present in the sediment. With the 60 mM initial concentration of dithionite, the rate of iron reduction was quite rapid (Figure 8). During the first 6 h, roughly 20 to 35% of the Fe(III) was reduced regardless of solid:solution ratio. At the highest solid:solution ratio (2.0) essentially no further Fe(III) reduction occurred. At lower solid:solution ratios, on the other hand, reduction of Fe(III) continued at a rapidly decreasing rate for the next several days. Even at the lowest solid:solution ratio (0.05), however, most of the Fe(III) (70% out of an eventual maximum of 77%) was reduced within the first 30 h of treatment. After 30 h, the levels of dithionite in all the solutions were still roughly one-half to one-third of their starting values, yet relatively little additional reduction of Fe(III) occurred. Unlike those of the dithionite decomposition reaction, the rates of Fe(III) reduction that were observed did not follow PFO kinetics. Rather, Fe(III) reduction seemed to follow a more complex mechanism that suggested that the ease of Fe(III) reduction became progressively more difficult (i.e., the activation energy increased) as the reaction progressed.

Such a progressive increase in activation energy is suggested by the log-linear relationship between the solid:solution ratio and the maximum amount of Fe(III) reduced by a 60 mM dithionite treatment (Figure 9). If the activation energy for the reaction remained constant, then a linear, rather than log-linear, relationship would be expected. The log-linear relationship that was observed might reflect a reaction front moving from the particle surface into the bulk of each particle, entailing longer and longer pathways for electron transfer from the bulk structural iron being reduced and the adsorbed reductant at the particle surface.

The occurrence of an activation-energy effect is also supported by calculations of the efficiency of structural iron reduction (Figure 10). It was assumed that the dithionite:iron reaction yields sulfite (rather than sulfate) as the oxidized form of dithionite. Reduction of the first 25 to 30% of the sediment iron proceeded at essentially 100% efficiency. This fraction of iron corresponds to the amount that is located in the clay-sized minerals (these minerals contain about 60 g iron kg^{-1}, and the clay content is also 60 g kg^{-1} soil), and this correspondence supports the premise that the iron in clays is the most readily reduced fraction. The efficiency of reduction decreased exponentially as larger fractions of the Fe(III) were reduced, such that nearly 15 times as much dithionite was required per mole of iron reduced to achieve 75% reduction as to achieve 25% reduction. The exponential nature of this relationship supports the concept of a progressive increase in activation energy associated with the mineral form of the iron. With a constant activation energy and no changes in other competing reactions, the efficiency of the reaction would remain constant.

Reoxidation of Reduced Sediment

Once the ability of dithionite to reduce the structural iron in sediments had been demonstrated, the next logical step was to demonstrate the utility of this reduced iron as a reductant for aqueous oxidized species under flowing conditions similar to those in an aquifer. This step was important because (1) colloidal transport of the reduced clay particles might decrease the effectiveness of the redox barrier [as noted by Gschwend and Wu (1985), reliance on batch experiments alone may cause the investigator to overlook significant colloidal transport processes], and (2) the rate at which the reduced iron would react with oxidized species in solution relative to the flow rate of the solution through the sediment is uncertain. A sufficiently slow rate (in comparison to the pore-water residence time) would mean that any simulations of the barrier efficacy and longevity must incorporate kinetic processes into the model. Alternatively, if the reoxidation rate were fast compared to the pore-water residence time, the behavior of the barrier at the field scale could be accurately modeled as an equilibrium process. Thus, the rate at which reduced structural iron in the clay was reoxidized by aqueous oxygen, which serves as a surrogate for inorganic oxidized contaminants such as chromate, may be controlled by a chemical kinetic step or by a physical process, such as diffusion in immobile pore water.

A series of one-dimensional column experiments was conducted to quantify the stoichiometry and the kinetics of the reoxidation of sediment that had been reduced by dithionite. Reaction stoichiometry was examined by determining the number of pore volumes of oxygen-saturated water needed to reoxidize the reduced sediment. The kinetics of this reoxidation process were examined by conducting experiments over a range of pore-water velocities, then fitting the data to several transport models that incorporated different assumptions about the kinetic processes involved.

Reoxidation Stoichiometry

The oxygen breakthrough curve for a typical column experiment is shown in Figure 11. In this particular experiment, reducing conditions were maintained by the iron until 110 pore volumes of initially oxygen-saturated water had pased through the column. Overall, the column experiments showed that reducing conditions were maintained for 40 to 190 pore volumes of oxygen-saturated water (Table 1). A mean value of about 83 pore volumes was obtained, which corresponds to about 2.3 μmol O_2 reduced per gram of sediment. Theoretical calculations based on the batch reduction results predicted much larger amounts of oxygen reduction. For example, conservatively assuming that 25% of the available Fe(III) was reduced by the dithionite treatment (Figures 8 and 10), about 54 μmol Fe(III) g^{-1} would be available for reaction with oxygen and would consume about 13 μmol O_2 g^{-1} of sediment. The variation in results among column experiments and between the column and batch experiments may reflect differences in (1) the amount of atmospheric oxygen diffusing into the columns during the study (the experiments were conducted in sealed columns, but under air on the benchtop), (2) the amount of reduced iron initially in the sediments, or (3) the amount of clay washed out of the sediment (i.e., colloid transport) by the treatment.

Reoxidation Rate

Three column experiments (3, 4, and 5 in Table 1) were conducted at different flow rates to obtain oxygen breakthrough data having different dependencies on chemical reaction kinetics relative to physical processes, such as diffusion. At the particle scale, the time required for diffusion (ordinary or Knudsen) into a porous particle would be significant only if the particles were large relative to the pore size and to the size of the solute molecule. Ordinary diffusion times vary with the square of the particle diameter and range from minutes for submillimeter-diameter particles to hours for centimeter-sized aggregates of particles. For the sieved sediment used in this study, all sediment particles were smaller than 2 mm dia, so the time for ordinary diffusion into these particles would be only a few minutes. Therefore, ordinary diffusion in immobile pore fluid was unlikely to affect the transport of solutes in flow systems with residence times of an hour or longer.

These experiments with shorter residence times (Figure 12) exhibited breakthrough behavior typical of a kinetically controlled process; namely considerably greater tailing at higher flow rates. This behavior depends on the relationship between the residence time in the column and the reaction time (often expressed in terms of a Damkohler number, Bahr and Rubin, 1987). As the flow rate increased, residence time in the column decreased. Given the same time of approach to equilibrium (i.e., reaction half-life for a chemical process) and faster flow rates, the efficiency of oxygen removal by the column decreased, which led to quicker breakthrough of a portion of the mass (Figure

12C) than in an equilibrium case (Figure 12A). During the later portions of breakthrough, the slow physical-chemical process continued and produced the slow approach to equilibrium observed in the oxygen breakthrough curve.

The experiment conducted at the fastest flow rate (Figure 12C) was fitted with a first-order model (the best fit is shown with the solid line) and with a two-region model (dashed line). The fit obtained with the first-order model was poor and implied that the kinetic process was more complex than a simple, first-order, reversible reaction. The two-region (i.e., two-reaction) model fit well to the shape of the breakthrough curve, indicating that the kinetic process(es) could be accounted for with this model. The tailing (i.e., slow approach to equilibrium) beyond 100 pore volumes, however, was not adequately fitted even with the two-region model. Further studies (e.g., spectroscopic studies of chemical reaction steps) would be required to identify the kinetic mechanism(s) completely.

The good fits obtained with the two-region model implied that the reoxidation process could be described by assuming a fraction of fast-reoxidation sites and a fraction of slow-reoxidation sites. Given the results of the batch experiments demonstrating different reduction efficiencies for different fractions of the Fe(III), this is the behavior during reoxidation that would be expected. Model fits to the two experiments run at faster flow rates (Figures 12B and 12C) indicated a mean fraction of fast sites of about 0.6. The PFO oxidation rate coefficients (k) for the two experiments were 0.15 h^{-1} and 0.24 h^{-1}, for a mean reaction half-life of 3.8 h. The mean fraction of fast sites ($f = 0.6$) and mean PFO rate coefficient ($k = 0.20\ h^{-1}$) were used in a third simulation with the two-region model for the experiment conducted at slow flow rates (Figure 12A). In this simulation the flow rate was so slow that the kinetic process was nearly at equilibrium and the fit of the two-region model was identical to that of the equilibrium model.

Given that reaction equilibrium can be assumed if residence time in the system is approximately two orders of magnitude greater than the reaction half-life (i.e., that the Damkohler number $\approx$ 100), equilibrium reoxidation can be assumed in flow systems with a residence time of 400 h or greater. Therefore, for most natural-gradient systems in the proposed remediation area, equilibrium reoxidation is sufficient to describe the behavior; in forced-gradient systems with fast flow rates, however, reoxidation kinetics would need to be included to accurately model the behavior.

In general, the reoxidation experiments demonstrated that a substantial reductive capacity could be stored in the structural iron of the sediments, and that this iron would react readily with oxygen, and presumably with other oxidized species such as chromate, under the flowing conditions encountered in aquifers. The mean value of the measured reductive capacity, however, was roughly six times smaller than was predicted from the batch experiments and the data were quite variable. Possible reasons for this discrepancy include the diffusion of air-derived oxygen into the columns during the experiment and the loss of iron-bearing clay particles by colloid transport during flow. Additional experiments under controlled atmospheric conditions are under way to help resolve this issue.

Abiotic Dechlorination of Tetrachloromethane

In addition to testing the efficacy of the dithionite-reduced iron in sediments to remove inorganic species (using oxygen as a surrogate), we examined whether the same process would act to remove chlorinated hydrocarbon species such as tetrachloromethane. An experiment was run involving untreated (i.e., oxidized) and dithionite-reduced sediment samples spiked with 0.50 μL CCl_4 L^{-1} suspension at 30°C. Precautions were taken to remove unreacted dithionite, sulfite, and thiosulfate ions from the soil system before adding the tetrachloromethane, and the entire experiment was conducted under an inert atmosphere.

The results of the experiment were quite encouraging (Figure 13). Within a week (168 h), roughly 90% of the CCl_4 had been destroyed by the reduced sediment. Only minor losses of CCl_4 occurred in the oxidized sediment during this period. Of the CCl_4 destroyed, only a small portion (<10%) had been converted to trichloromethane, and dichloromethane levels were at or below detection limits. Although the exact nature of the reaction products has not been established, these results suggest that other volatile chlorinated hydrocarbons are not created to any significant extent by the reaction of tetrachloromethane with reduced sediment. The rate of reduction could be fitted to PFO kinetics (Figure 14) and yielded a PFO rate constant of 1.4E-2 h^{-1} ($t_{1/2}$ = 48 h). These dechlorination rates compare favorably with those ($\approx$ 1.0E-2 h^{-1}) reported by Kriegman-King and Reinhard (1994) for reactions of CCl_4 with pyrite (FeS_2). However, Kriegman-King and Reinhard observed a zero-order reaction (k = 2.1-5.3E-2 mol m^{-2} d^{-1}) rather than the PFO reaction observed in our experiments. The difference in reaction order suggests that the mechanisms in the two systems are fundamentally different. It may be that the pyrite system involves the leaching of iron from the structure and the formation of sulfide intermediates (Kriegman-King and Reinhard, 1994), whereas the iron in layer silicates remains in the mineral structure when reoxidized and, so far as we can determine, no sulfur species are involved.

Feasibility of Large-Scale In-Situ Dithionite Treatments

There can be little doubt that dithionite will be able to reduce a zone in an aquifer containing iron-bearing layer silicates. The main questions at this point relate to the desired longevity of such a barrier (i.e., how much iron will have to be reduced) and the most effective concentration of dithionite to achieve a sufficient level of reduction (i.e., the efficiency of the reduction process). Using dissolved oxygen as an analog for chromate, it seems clear that a reduced barrier could be effective for a long period of time, possibly several years, depending on the groundwater flow rate.

ACKNOWLEDGMENTS

Much preliminary research was performed by Robert A. Speed while on a Science and Engineering Research Semester (SERS) appointment funded by the U. S. Department of Energy, and by one of us (JCT) while on a sabbatical leave funded by Whitman College and by the U. S. Department of Energy. We thank Gary P. Turner, Steven C. Smith, and Joseph P. Zipperer, all of the Pacific Northwest Laboratory, for technical assistance. This work was funded by the

Office of Technology Development, within the U. S. Department of Energy's Office of Environmental Restoration and Waste Management, under the In Situ Remediation Technology Development Integrated Program (ISRIP). We thank Mary E. Peterson, ISRIP program manager, and Jef Walker, ISRIP program director, for their continuing support and encouragement. Pacific Northwest Laboratory is operated for the U. S. Department of Energy by Battelle Memorial Institute under Contract DE-AC06-76RLO 1830.

REFERENCES

Anderson, LD, DB Kent, and JA Davis. **1994.** Batch experiments characterizing the reduction of Cr(VI) using suboxic material from a mildly reducing sand and gravel aquifer. Environ Sci Technol 28:178-185.

Bahr, J and J Rubin. **1987.** Direct comparison of kinetic and local equilibrium formulations for solute transport affected by surface reactions. Water Resour Res 23:438-452.

Creutz, C and N Sutin. **1974.** Kinetics of the reactions of sodium dithionite with dioxygen and hydrogen peroxide. Inorg Chem 13:2041-2043.

Gschwend, PM and S Wu. **1985.** On the constancy of sediment-water partition coefficient of hydrophobic organic pollutants. Environ Sci Technol 19:90-96.

Horvath, C and H Lin. **1978.** Band spreading in liquid chromatography. J Chromatogr 149:43-70.

Kent, DB, JA Davis, LD Anderson, BA Rea, and TD Waite. **1994.** Transport of chromium and selenium in the suboxic zone of a shallow aquifer. Water Resour Res 28:1099-1114.

Komadel, P and JW Stucki. **1988.** Quantitative assay of minerals for Fe^{2+} and Fe^{3+} using 1,10-phenanthroline--III. A rapid photochemical method. Clays Clay Miner 36:379-381.

Kriegman-King, MR and M Reinhard. **1994.** Transformation of carbon tetrachloride by pyrite in aqueous solution. Environ Sci Technol 28:692-700.

Parker, J and MTh van Genuchten. **1984.** Determining Transport Parameters from Laboratory and Field Tracer Experiments, Virginia Agric. Exp. Stn. Bull. 84-3, Blacksburg, VA.

Rose, D. **1977.** Hydrodynamic dispersion in porous materials. Soil Sci 123:277-283.

Scott, AD and JE Amonette. **1988.** Role of iron in mica weathering, pp. 537-623. In: Iron in Soils and Clay Minerals, JW Stucki, BA Goodman, and U Schwertmann, eds. D Reidel, Dordrecht, The Netherlands.

Stucki, JW. **1988.** Structural iron in smectites, pp. 625-675. In: Iron in Soils and Clay Minerals, JW Stucki, BA Goodman, and U Schwertmann, eds. D Reidel, Dordrecht, The Netherlands.

Szecsody, JE and RC Bales. **1989**. Sorption kinetics of low-molecular-weight hydrophobic organic compounds on surface-modified silica. J Contam Hydrol 4:181-203.

Templeton, JC, JR Nelson, and JE Amonette. **1994**. Improvements in the quantitative assay of nonrefractory minerals for Fe(II) and total Fe using 1,10-phenanthroline. <u>Program and Abstracts, 49th Northwest Regional Meeting of the American Chemical Society, June 16-18, 1994, Anchorage, Alaska</u>, American Chemical Society, Washington, DC.

Table 1. Summary of column-experiment data for reoxidation of reduced Hanford Site sediment by oxygen-saturated simulated Hanford groundwater.

		Flow Rate		Oxygen Breakthrough Time,	
Experiment	Pore Volume, cm^3	Pore-Water Velocity, cm h^{-1}	Effluent Velocity, PV h^{-1}	h	PV(a)
1	12.	5.0	1.0	49.	50
2	12.	4.2	0.84	220.	190
3	4.8	4.8	2.4	45.	110
4	4.8	32.	16.	4.3	68
5	4.8	12.	5.9	7.9	47
6	4.8	3.8	1.9	21.	41

(a) Pore Volumes

Figure Captions

Figure 1. Absorption spectra of aqueous sulfate (SO_4^{2-}), sulfite (SO_3^{2-}), thiosulfate ($S_2O_3^{2-}$) and dithionite ($S_2O_4^{2-}$) ions and (inset) the structure and bond lengths of the dithionite ion.

Figure 2. Some possible chemical reactions associated with treatment of sediments by aqueous dithionite solutions. In addition to production of sulfoxyl free radical ($SO_2^{\bullet-}$) and disproportionation to yield sulfite (SO_3^{2-}), thiosulfate ($S_2O_3^{2-}$), and protons, the transfer of electrons to structural iron in clays and, subsequently, to oxidized species is shown as well as associated precipitation and adsorption reactions.

Figure 3. Changes in aqueous concentration of dithionite ion in simulated Hanford groundwater solutions buffered at pH 8 and incubated at 30°C under anoxic conditions. Two initial concentrations (60 and 2.2 mM) of dithionite were used, yielding half-lives of 135 and 243 h, respectively.

Figure 4. Changes in aqueous concentrations of dithionite, measured under identical conditions for sediments that either were prereduced or remained oxidized before treatment with dithionite. Experiments conducted using 60 mM starting concentrations of dithionite, a 1:1 solid:solution ratio, and incubation at 30°C under anoxic conditions. Reaction half-lives calculated assuming pseudo-first-order kinetics were 19 and 24 h for prereduced and oxidized

samples, respectively, and were not significantly different at 95% level of probability.

Figure 5. Changes in aqueous concentrations of dithionite measured during the first 10 h of contact with sediments that either were prereduced or remained oxidized before treatment. Experiments were conducted using 60 mM starting concentrations of dithionite, a 1:1 solid:solution ratio, and incubation at 30°C under anoxic conditions.

Figure 6. Pseudo-first-order (PFO) rate plot for decomposition of aqueous dithionite ions in contact with Hanford sediment at 30°C under anoxic conditions and a solid:solution ratio of 0.5. Three initial concentrations of dithionite were used (62, 13, and 2.7 mM), yielding PFO half-lives of 36, 6.5, and 1.2 h, respectively.

Figure 7. Effect of solid:solution ratio on half-life of aqueous dithionite in contact with Hanford sediment at 30°C under anoxic conditions. Half-life of dithionite in absence of sediment (homogeneous solution) is also shown. Initial concentration of dithionite was 60 mM in all experiments.

Figure 8. Changes in the amount of Fe(III) in Hanford sediment arising from treatment by aqueous 60 mM dithionite solutions at different solid:solution ratios. Experiments conducted at 30°C under anoxic conditions.

Figure 9. Log-linear relationship between maximum amount of Fe(III) reduced in Hanford sediment by dithionite treatment and solid:solution ratio. Initial dithionite concentrations of 60 mM used in all experiments; samples incubated at 30°C under anoxic conditions.

Figure 10. Changes in average efficiency of Fe(III) reduction in Hanford sediment by aqueous dithionite solutions relative to maximum amount of Fe(III) reduced by treatments.

Figure 11. Changes in dissolved oxygen levels measured in effluent from typical column study of reoxidation of Hanford sediment reduced by dithionite treatment. Experiment conducted using oxygen-saturated, simulated, Hanford groundwater at room temperature (RT) and flow rate of 2.4 pore volumes h^{-1}.

Figure 12. Effluent concentrations of dissolved oxygen measured in column studies at flow rates of A, 2.4 pore volumes h^{-1}; B, 5.9 pore volumes h^{-1}; and C, 16 pore volumes h^{-1}, and fits of reaction models assuming equilibrium, first-order kinetics, or a combination of fast and slow reactions (two-region). Experiments conducted at room temperature using oxygen-saturated, simulated, Hanford groundwater.

Figure 13. Changes in concentrations of CCl_4 and $CHCl_3$ measured in sealed bottles containing oxidized sediment or sediment that had been prereduced by dithionite and washed free of reductants. Experiment conducted at 30°C under anoxic conditions with 1 g

sediment in 5 mL of filtered anoxic Hanford groundwater. Initial concentrations of CCl_4 and $CHCl_3$ were 0.5 and 0.0 $\mu L\ L^{-1}$, respectively.

Figure 14. Pseudo-first-order rate plot of loss of CCl_4 in sealed bottles containing prereduced sediment at 30°C. Experimental conditions same as in Figure 13.

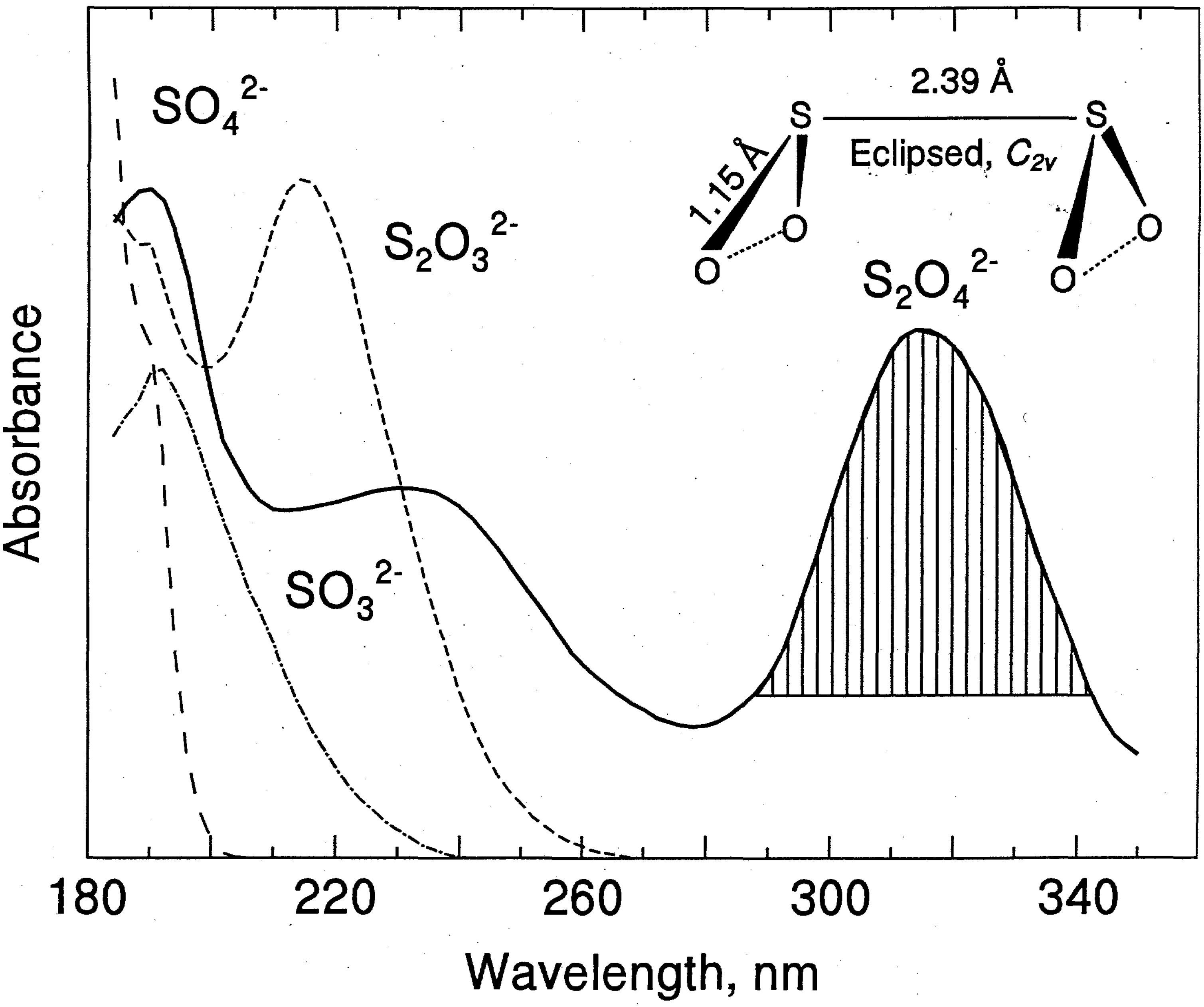
SO_4^{2-}
$S_2O_3^{2-}$
SO_3^{2-}
$S_2O_4^{2-}$
2.39 Å
S
S
1.15 Å
Eclipsed, C_{2v}
O
O
O
O
Absorbance
180
220
260
300
340
Wavelength, nm

①

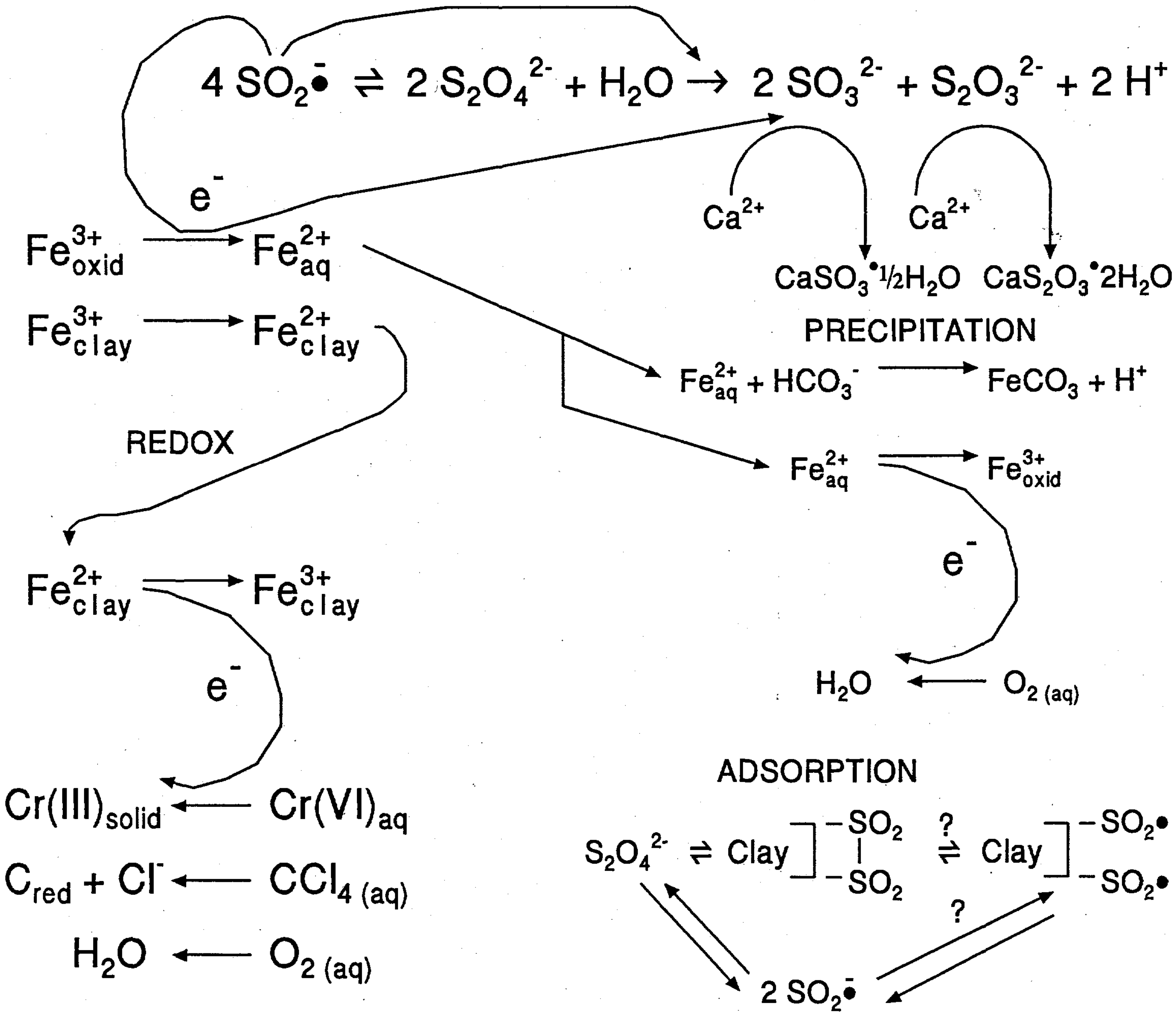
$4\,SO_2^{\bullet-} \rightleftharpoons 2\,S_2O_4^{2-} + H_2O \rightarrow 2\,SO_3^{2-} + S_2O_3^{2-} + 2\,H^+$
e^-
$Fe^{3+}_{oxid} \rightarrow Fe^{2+}_{aq}$
$Fe^{3+}_{clay} \rightarrow Fe^{2+}_{clay}$
REDOX
$Fe^{2+}_{clay} \rightarrow Fe^{3+}_{clay}$
e^-
$Cr(III)_{solid} \leftarrow Cr(VI)_{aq}$
$C_{red} + Cl^- \leftarrow CCl_{4\,(aq)}$
$H_2O \leftarrow O_{2\,(aq)}$
Ca^{2+}
Ca^{2+}
$CaSO_3 \cdot {}^1\!/\!_2H_2O$
$CaS_2O_3 \cdot 2H_2O$
PRECIPITATION
$Fe^{2+}_{aq} + HCO_3^- \rightarrow FeCO_3 + H^+$
$Fe^{2+}_{aq} \rightarrow Fe^{3+}_{oxid}$
e^-
$H_2O \leftarrow O_{2\,(aq)}$
ADSORPTION
$S_2O_4^{2-} \rightleftharpoons$ Clay $-SO_2$ | $-SO_2$
?
$\rightleftharpoons$ Clay $-SO_2^{\bullet}$ $-SO_2^{\bullet}$
?
$2\,SO_2^{\bullet-}$

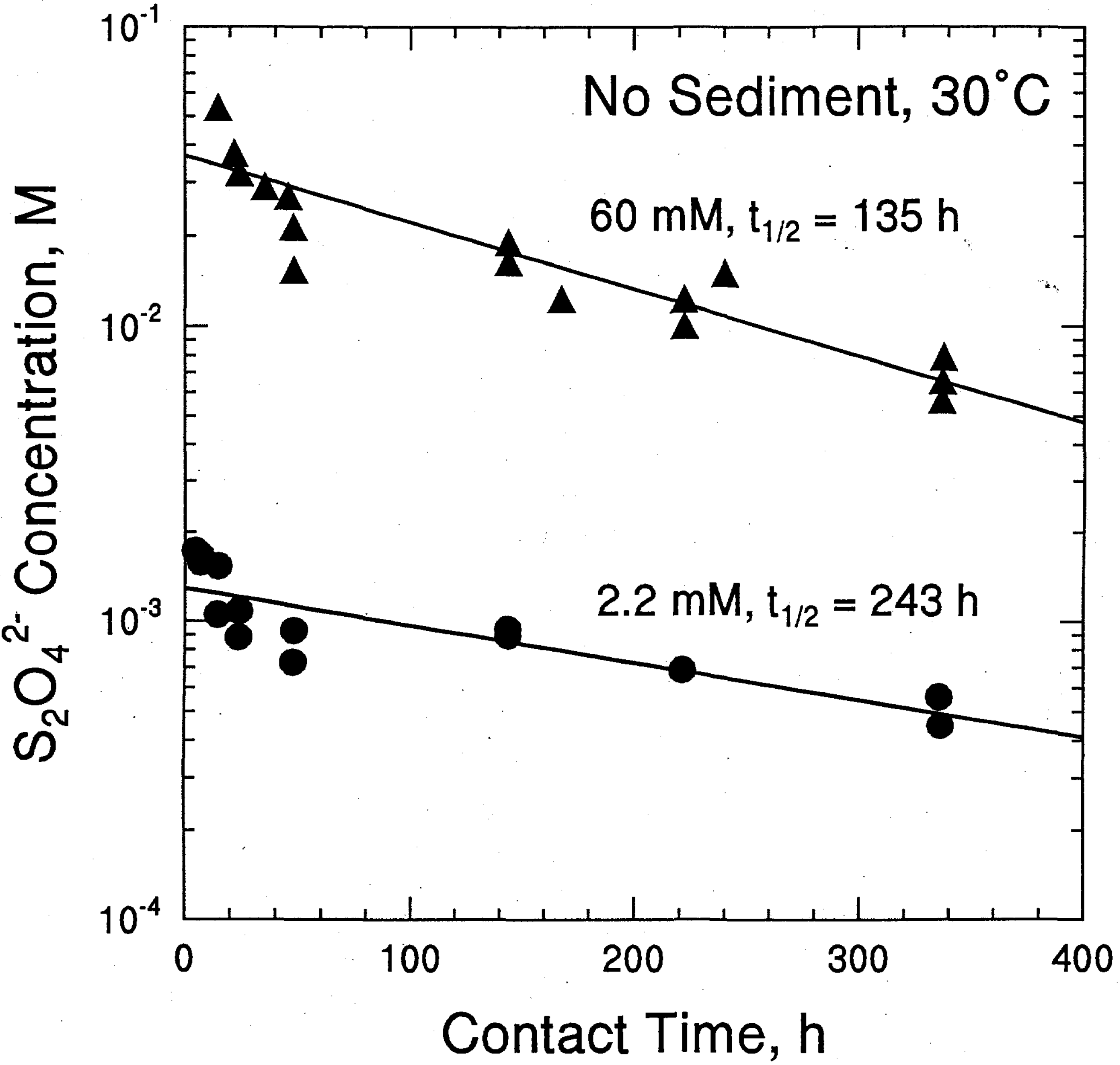

No Sediment, 30°C
60 mM, $t_{1/2}$ = 135 h
2.2 mM, $t_{1/2}$ = 243 h
$S_2O_4^{2-}$ Concentration, M
Contact Time, h
10^{-1}
10^{-2}
10^{-3}
10^{-4}
0
100
200
300
400

③

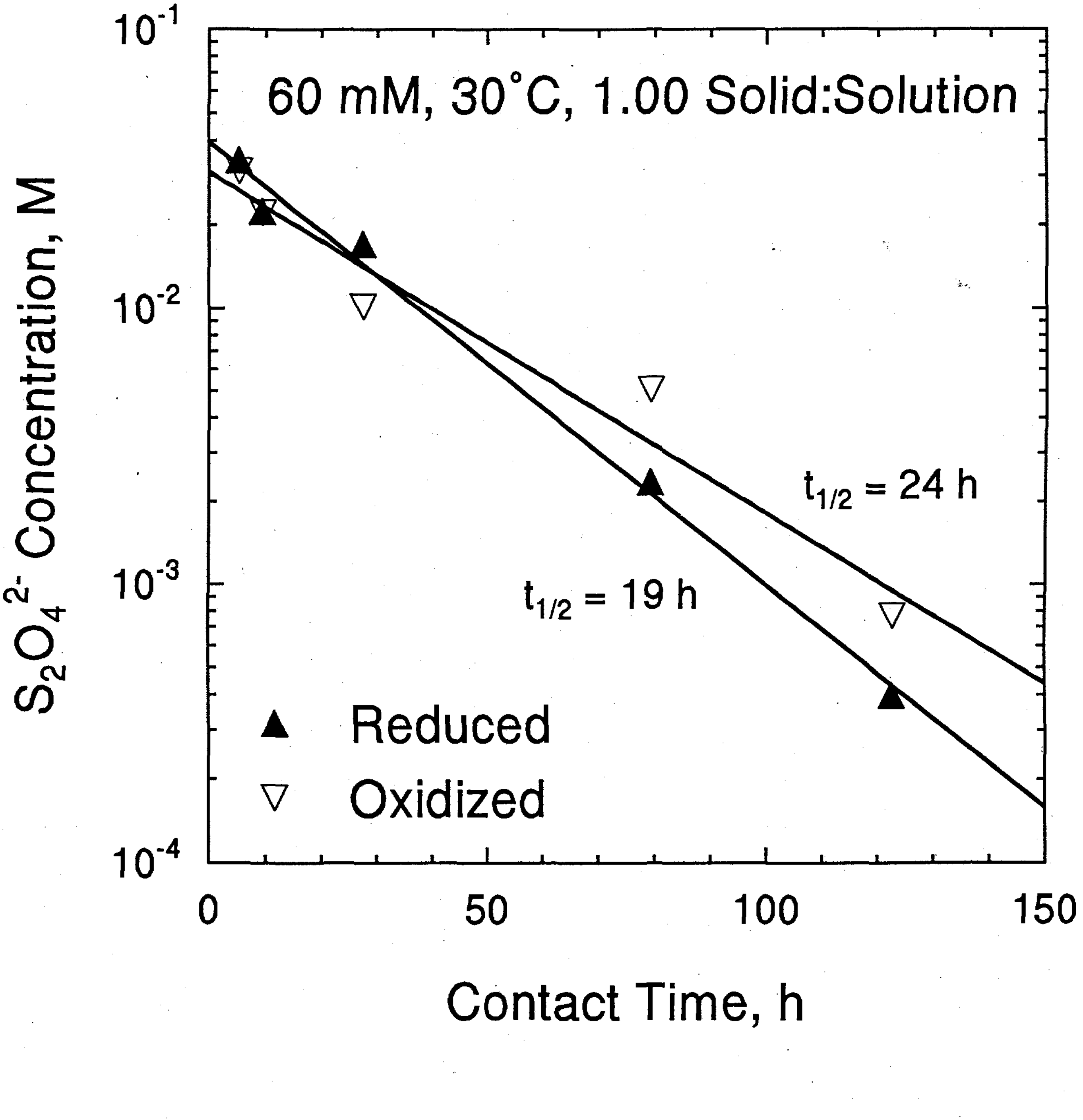

60 mM, 30°C, 1.00 Solid:Solution
$S_2O_4^{2-}$ Concentration, M
10^{-1}
10^{-2}
10^{-3}
10^{-4}
$t_{1/2}$ = 24 h
$t_{1/2}$ = 19 h
▲ Reduced
▽ Oxidized
0
50
100
150
Contact Time, h

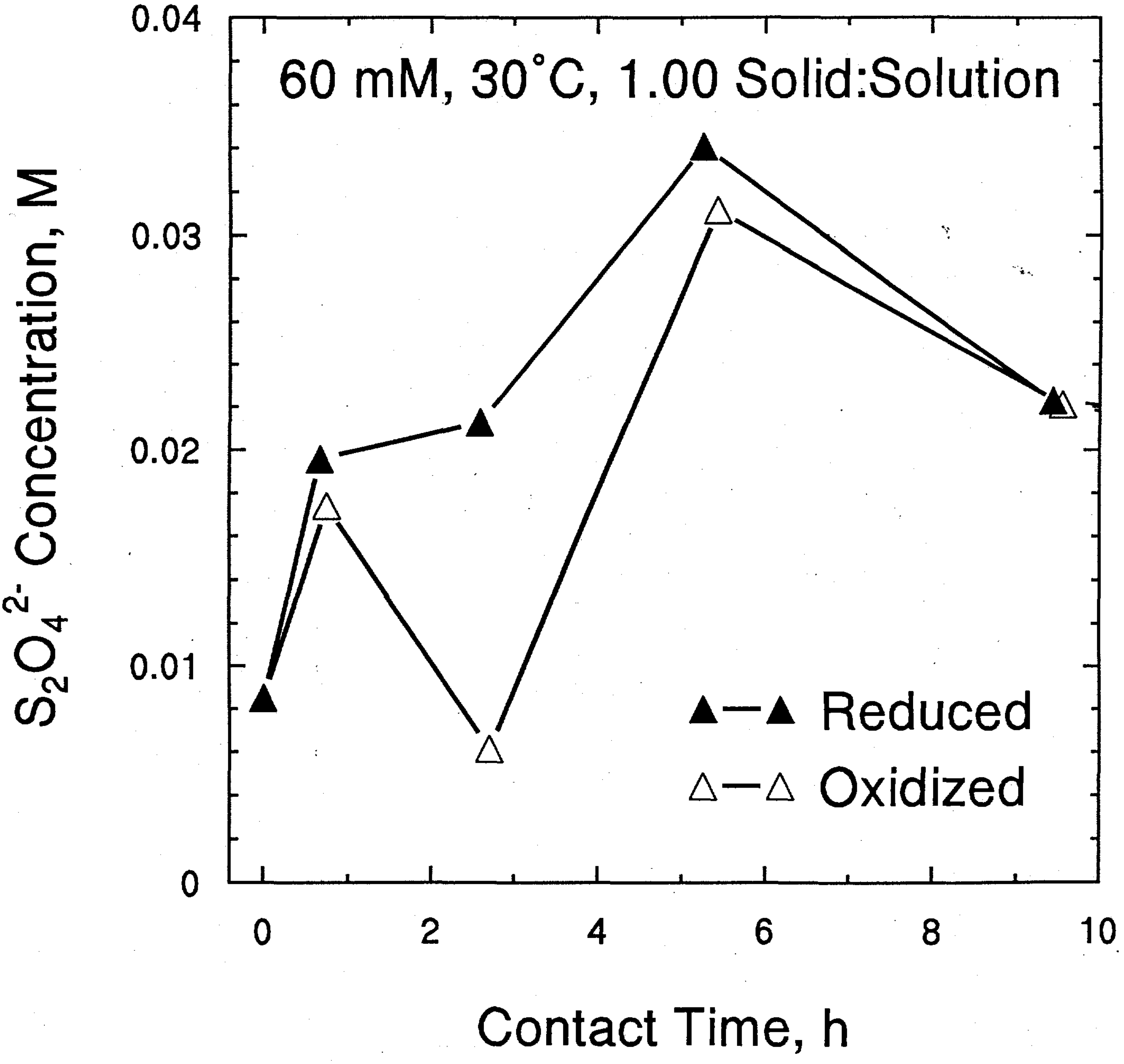
60 mM, 30°C, 1.00 Solid:Solution
$S_2O_4^{2-}$ Concentration, M
0.04
0.03
0.02
0.01
0
0
2
4
6
8
10
Contact Time, h
▲—▲ Reduced
△—△ Oxidized

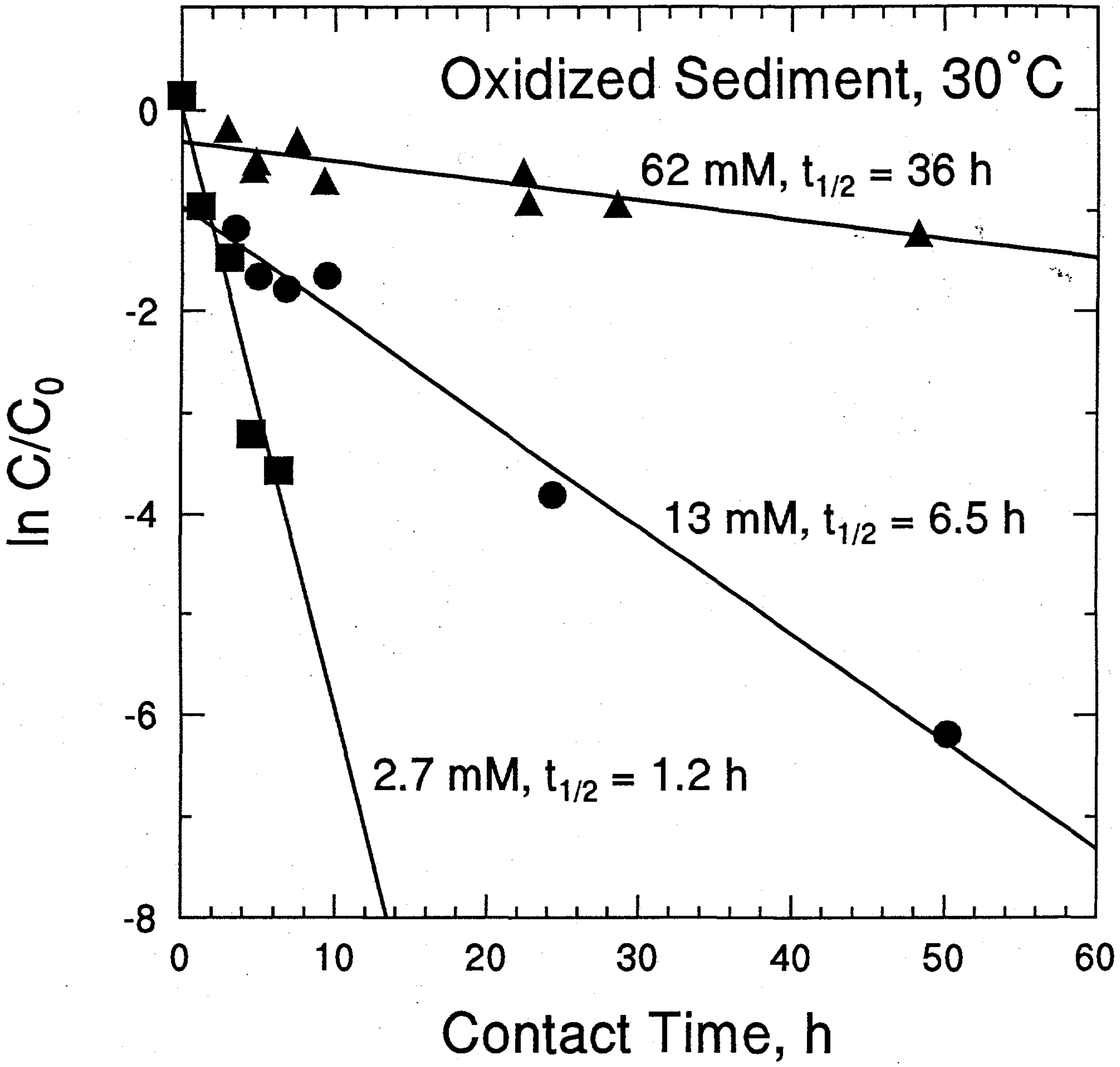
Oxidized Sediment, 30°C
62 mM, $t_{1/2}$ = 36 h
13 mM, $t_{1/2}$ = 6.5 h
2.7 mM, $t_{1/2}$ = 1.2 h
ln C/C_0
0
-2
-4
-6
-8
0
10
20
30
40
50
60
Contact Time, h

⑥

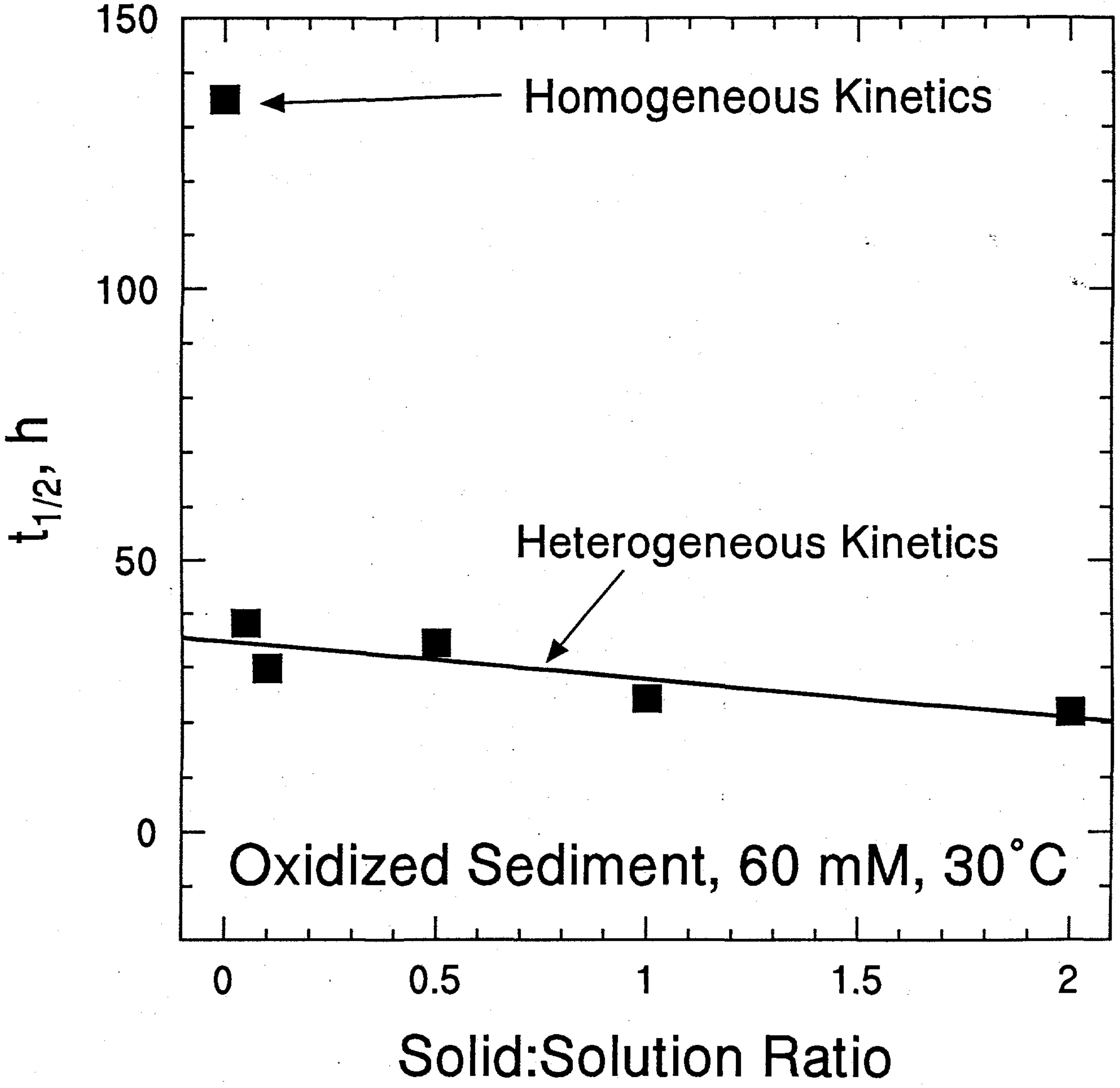
150
100
50
0
$t_{1/2}$, h
Homogeneous Kinetics
Heterogeneous Kinetics
Oxidized Sediment, 60 mM, 30°C
0
0.5
1
1.5
2
Solid:Solution Ratio

(9)

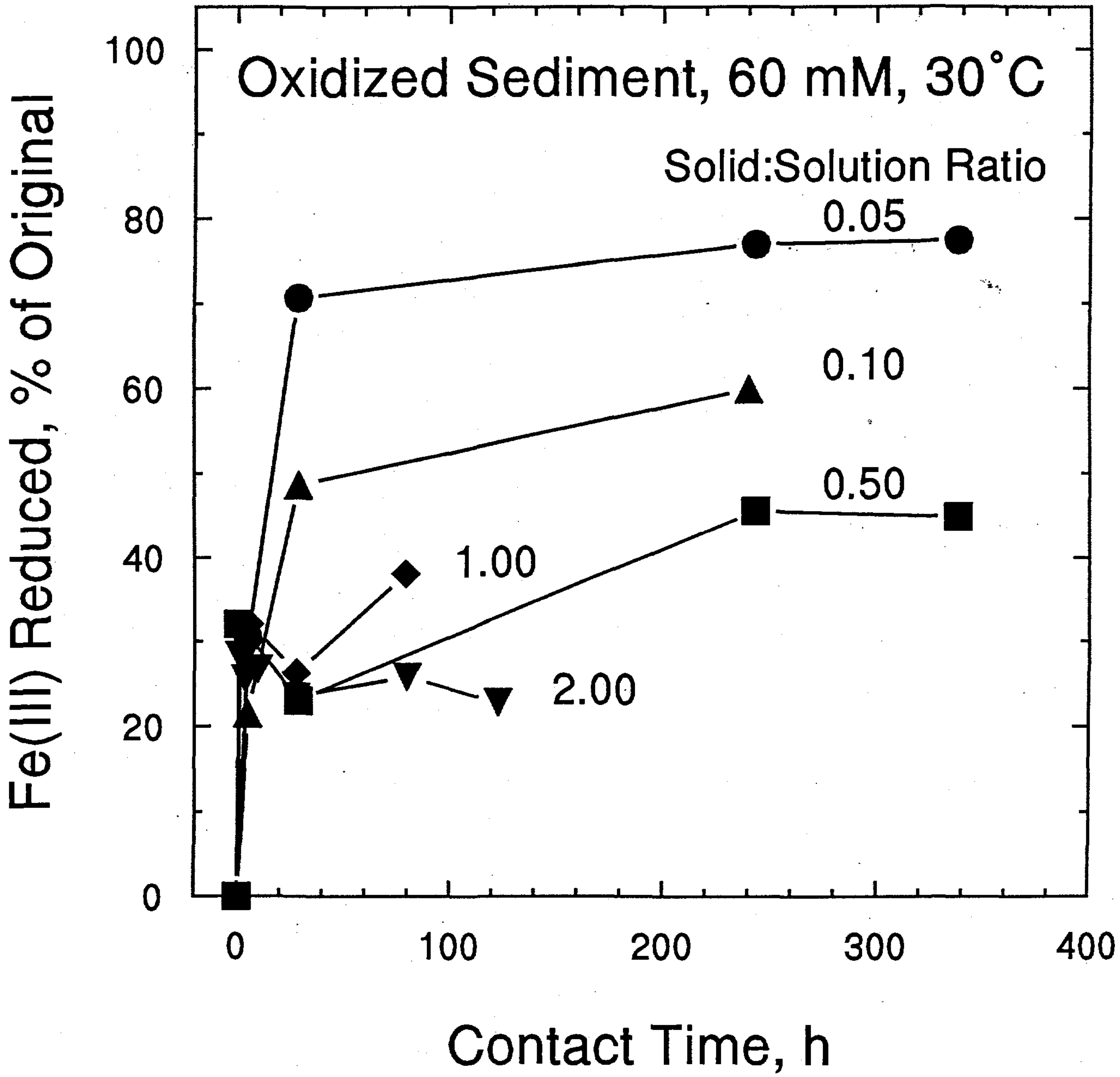
Oxidized Sediment, 60 mM, 30˚C
Solid:Solution Ratio
0.05
0.10
0.50
1.00
2.00
Fe(III) Reduced, % of Original
0
20
40
60
80
100
0
100
200
300
400
Contact Time, h

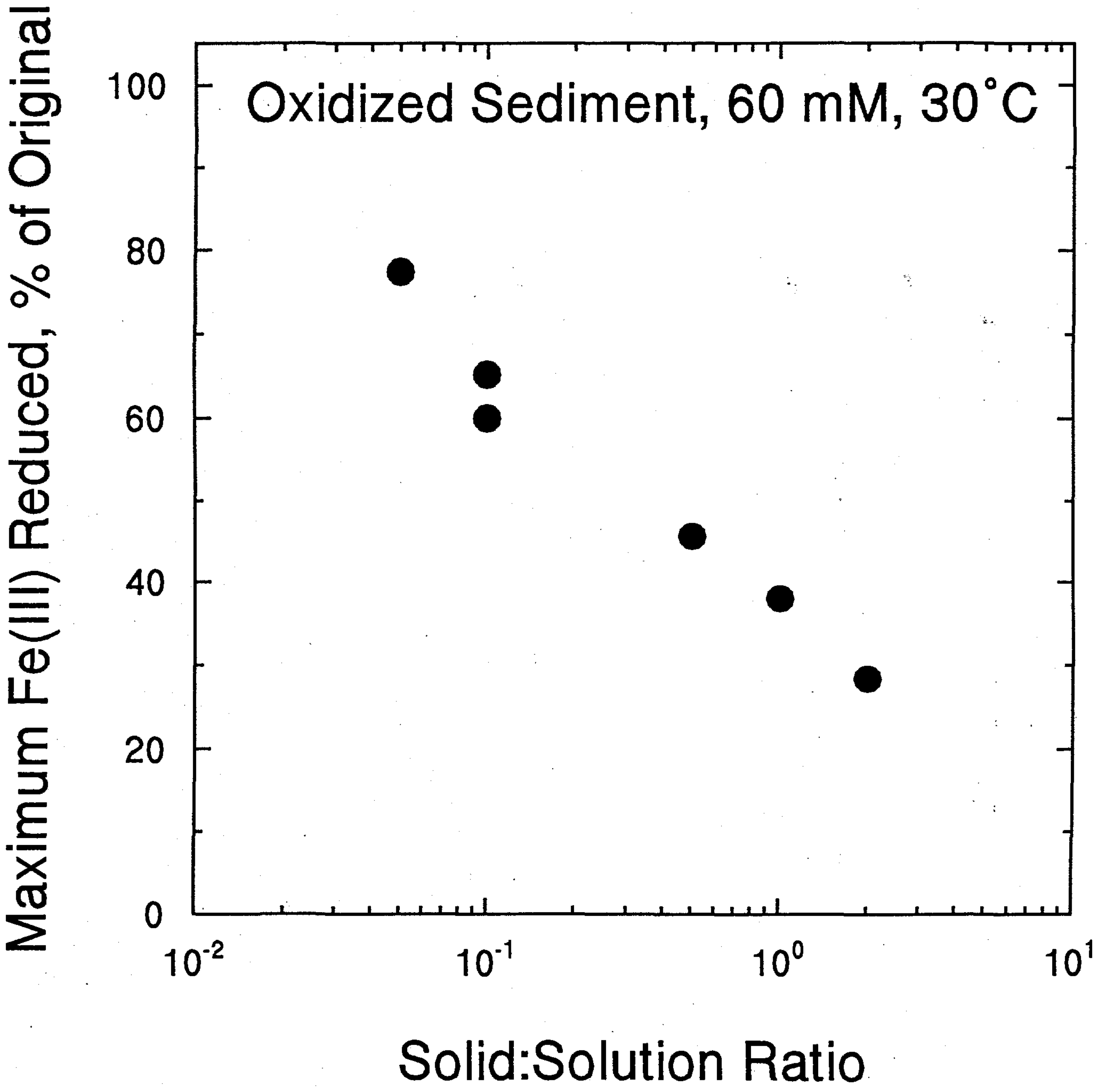
Oxidized Sediment, 60 mM, 30°C
Maximum Fe(III) Reduced, % of Original
0
20
40
60
80
100
10^{-2}
10^{-1}
10^{0}
10^{1}
Solid:Solution Ratio

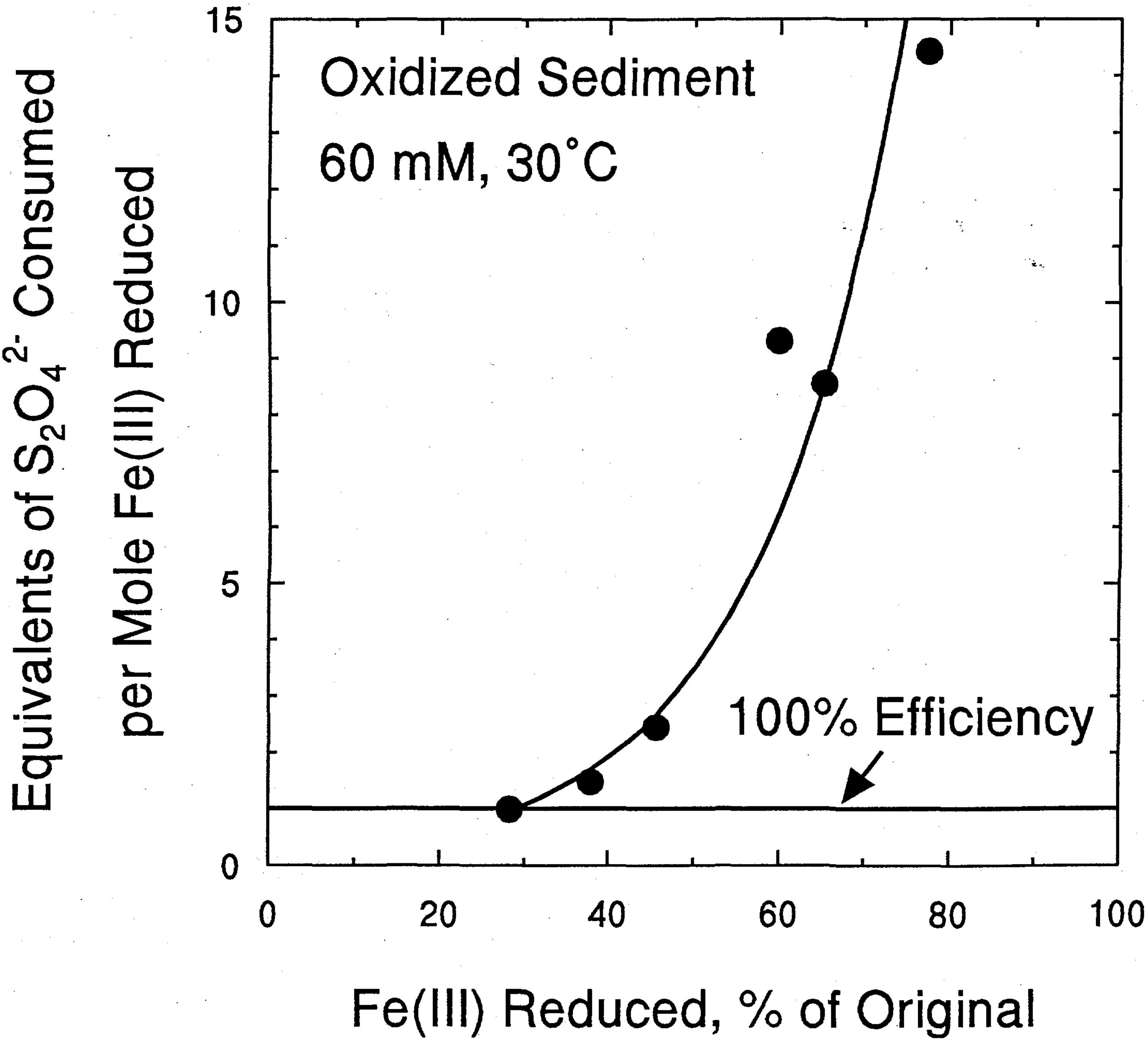
Oxidized Sediment
60 mM, 30°C
100% Efficiency
Equivalents of $S_2O_4^{2-}$ Consumed per Mole Fe(III) Reduced
Fe(III) Reduced, % of Original
0
5
10
15
0
20
40
60
80
100

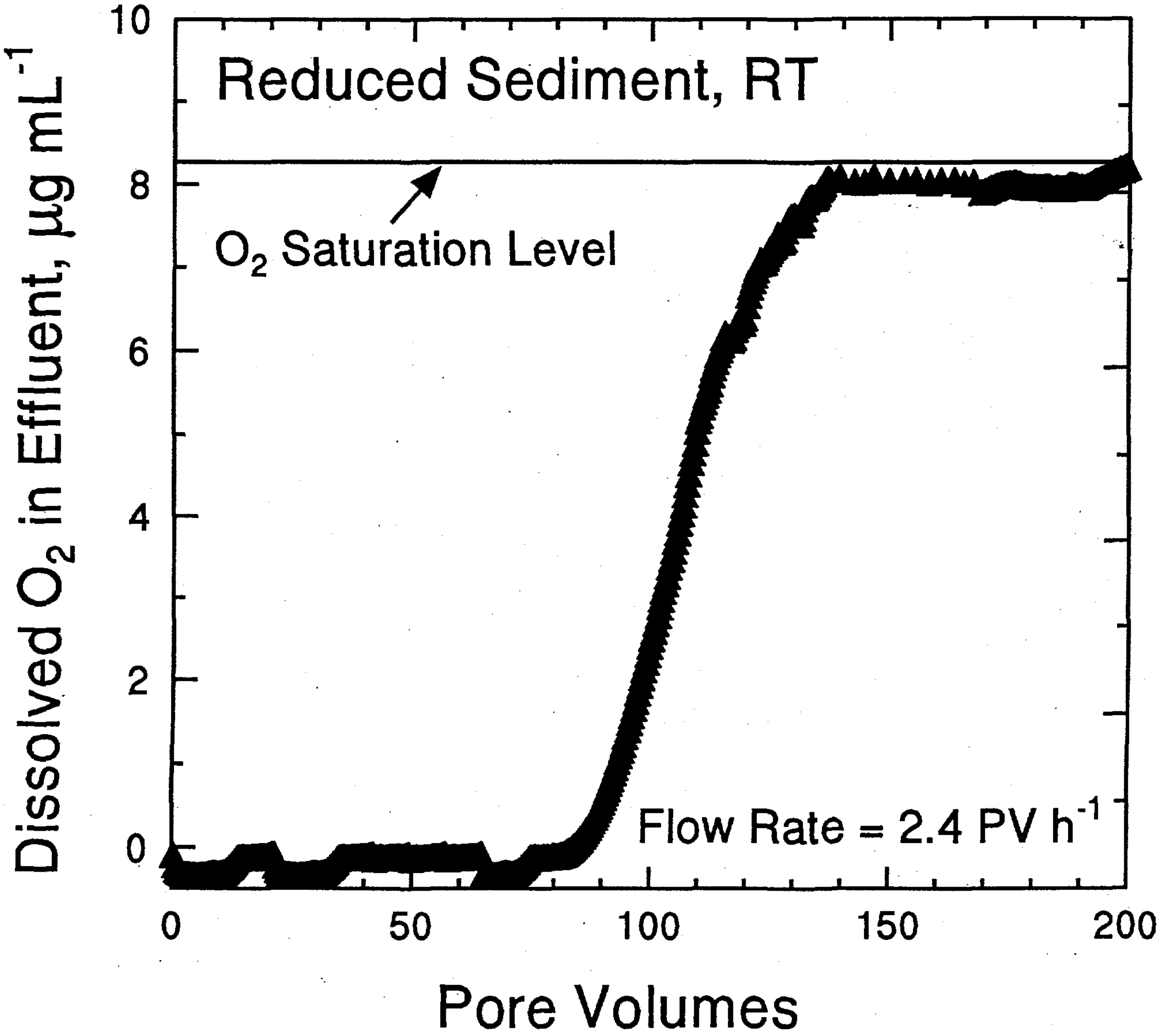
Reduced Sediment, RT
O$_2$ Saturation Level
Flow Rate = 2.4 PV h^{-1}
Dissolved O$_2$ in Effluent, μg mL^{-1}
Pore Volumes
0
2
4
6
8
10
0
50
100
150
200

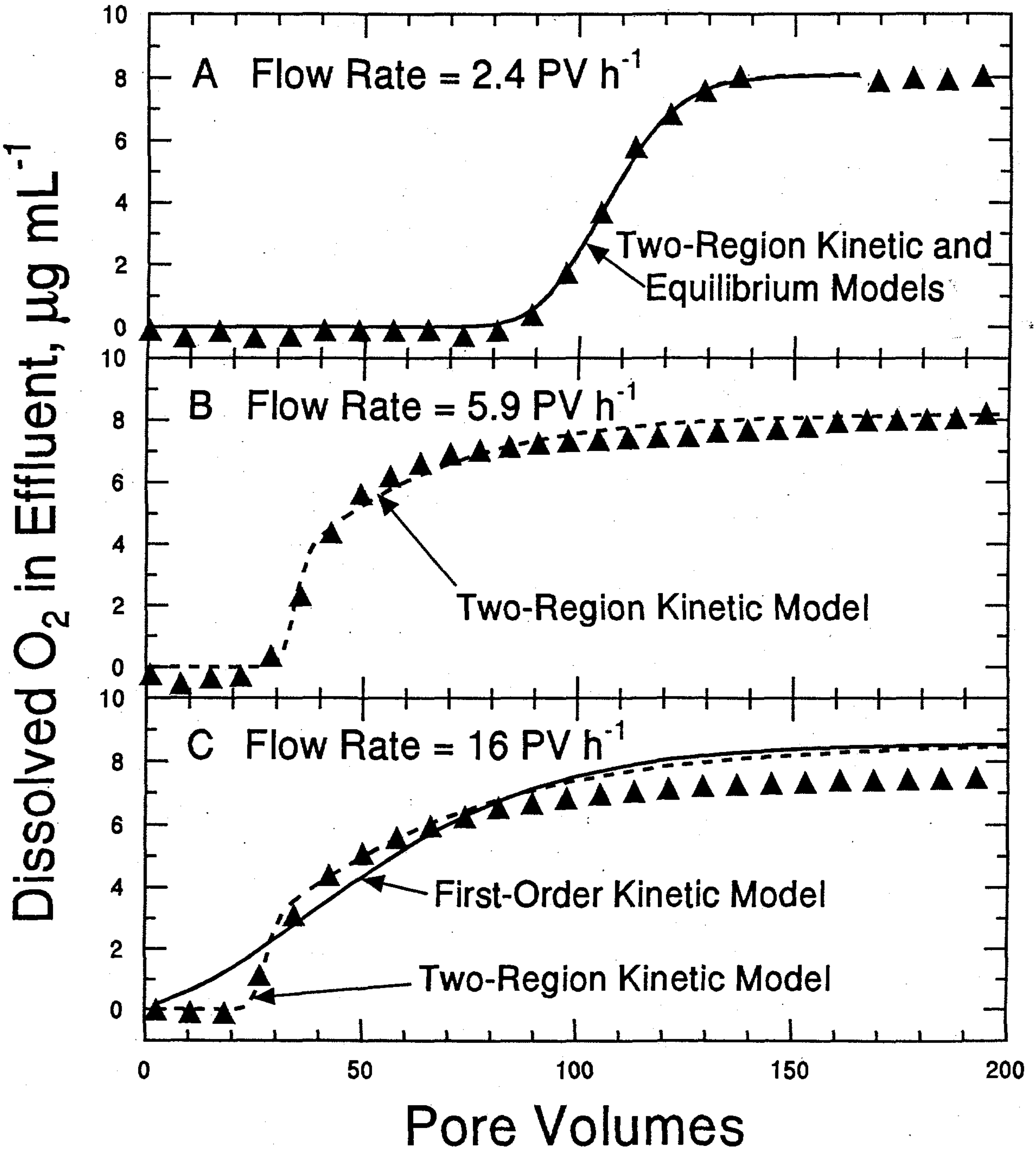
A Flow Rate = 2.4 PV h^{-1}
Two-Region Kinetic and Equilibrium Models
B Flow Rate = 5.9 PV h^{-1}
Two-Region Kinetic Model
C Flow Rate = 16 PV h^{-1}
First-Order Kinetic Model
Two-Region Kinetic Model
Dissolved O_2 in Effluent, µg mL^{-1}
0
2
4
6
8
10
0
50
100
150
200
Pore Volumes

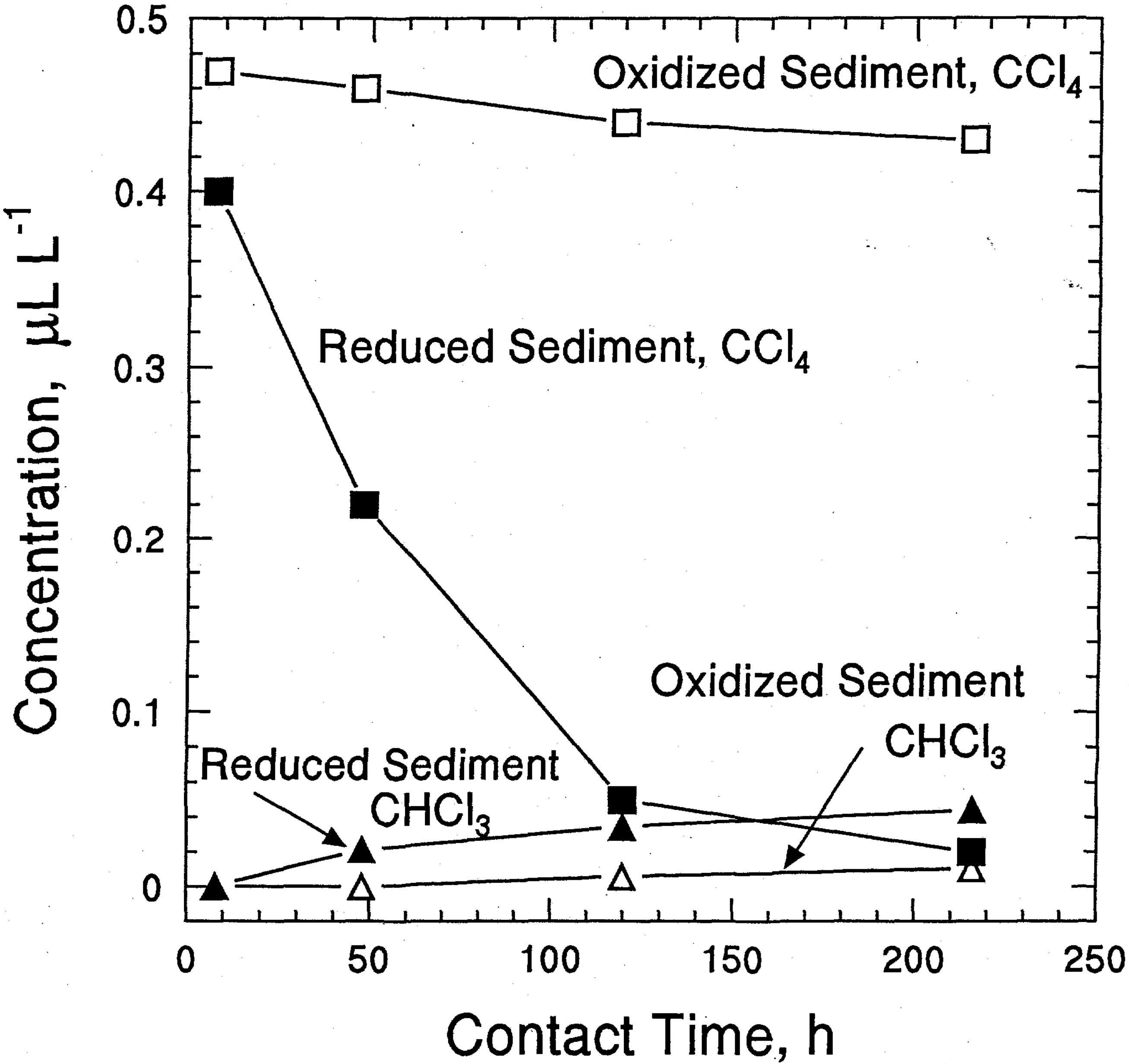

0.5
0.4
0.3
0.2
0.1
0
Concentration, $\mu L\ L^{-1}$
0
50
100
150
200
250
Contact Time, h
Oxidized Sediment, CCl_4
Reduced Sediment, CCl_4
Oxidized Sediment
$CHCl_3$
Reduced Sediment
$CHCl_3$

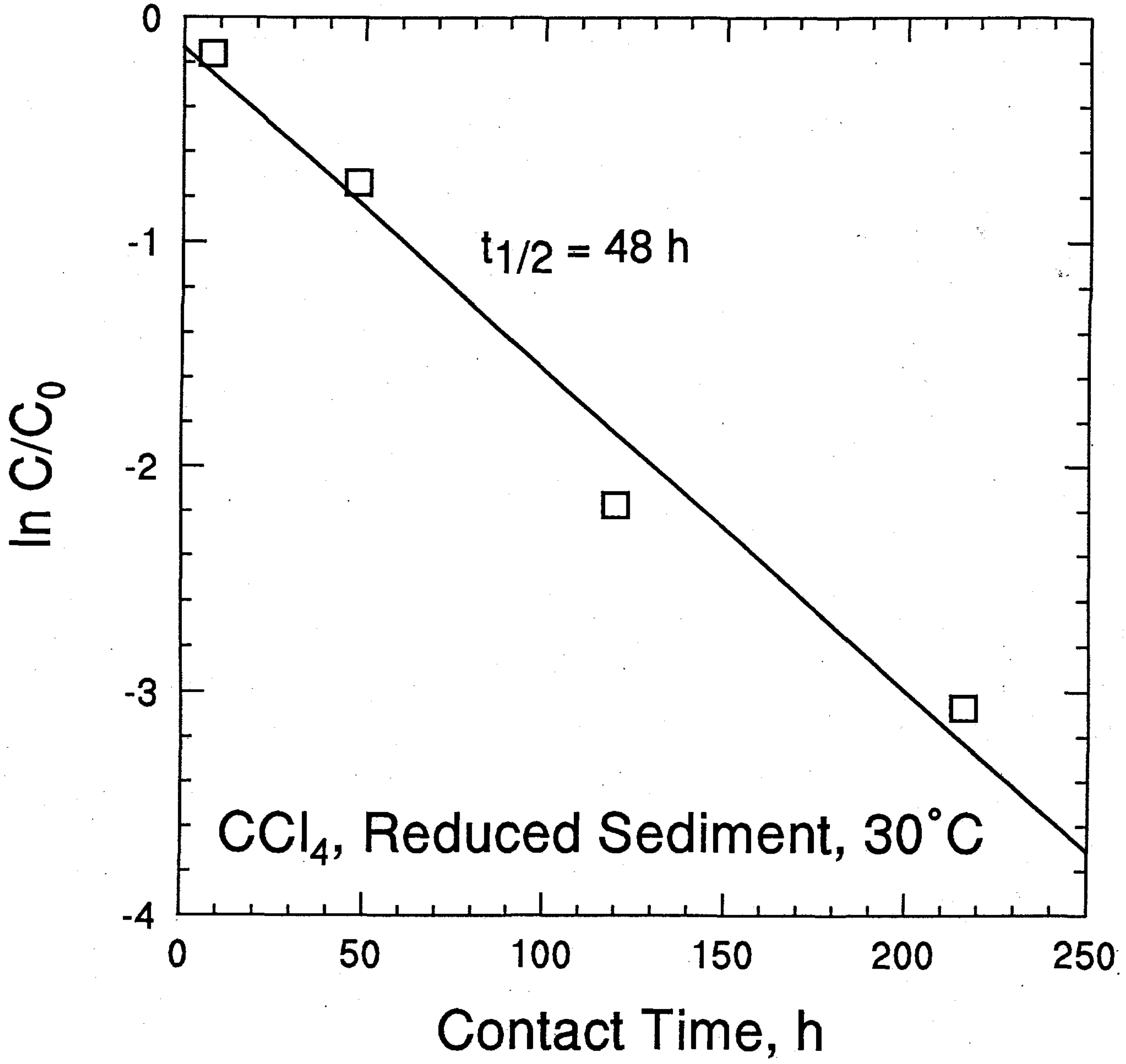

0
-1
-2
-3
-4
ln C/C_0
$t_{1/2}$ = 48 h
CCl_4, Reduced Sediment, 30°C
0
50
100
150
200
250
Contact Time, h